



Norwegian University of  
Science and Technology

# Microarrays for High Throughput Analysis of Cellular Heterogeneity

**Karen Dunker**

Biotechnology (5 year)

Submission date: August 2017

Supervisor: Marit Sletmoen, IBT

Norwegian University of Science and Technology  
Department of Biotechnology and Food Science



## Summary

The importance of cellular heterogeneity within cell populations has been increasingly realized in recent years. As a result, there has been a focus on developing methods for single cell analysis.  $\mu$ CP represents a cheap, simple and versatile method for producing microarrays across a substrate surfaces. The microarrays can be utilized for cell immobilization, which can be coupled to microscopy techniques. There is also an increased interest in using AFM for cell studies, which requires immobilization

The focus of this thesis was to develop a method for  $\mu$ CP of PLL to facilitate immobilization of *S. cerevisiae* on a glass substrate. The idea is to create a pattern that enables immobilization of single cells of *S. cerevisiae* to achieve SCA.

A photolithography procedure was developed to create a master mould for replica moulding. An even film thickness was achieved, but there were persistent problems with edge bead and cracks in the resist due to thermal stress. Replica moulding was used to make PDMS stamps on the created master mould. AFM analysis showed irregularities in the stamps corresponding to the cracks observed in the resist, which resulted in poor conformal contact between the stamp and the substrate surface. The parameters of the replica moulding method were verified using a pre-made master mould to create stamps. This showed that the process was suitable for creating PDMS stamps with micrometre scale features. The stamps were used to demonstrate that PDMS stamps could be used to print PLL in a micrometre scale pattern.

It was also demonstrated that *S. cerevisiae* could be immobilized on glass substrates functionalized with PLL.



## Samandrag

Det har vore ei auka forståing av viktigheta av cellulær heterogenitet i cellepopulasjonar i seinare år. Som eit resultat av dette har det vorte eit fokus på å utvikle metodar for enkeltcelle-analyse.  $\mu$ CP er ein billig, enkel og fleksibel metode for å produsere mikro-array på substratoverflater. Mikro-array kan brukast for immobilisering av celler, noko som kan koplast til mikroskopi for å studere enkeltceller. Det er også ei auka interesse for å bruke AFM til cellestudier, noko som krever immobilisering.

Fokuset for oppgåva var å utvikle ein metode for  $\mu$ CP av PLL for å fasilitere immobilisering av *S. cerevisiaea* på ei mønstra glassoverflate. Ideen er å lage eit mønster som mogleggjer binding av enkeltceller av *S. cerevisiae* slik at ein kan utføre enkeltcelle-analyse.

Ei fotolitografi-prosedyre for å lage ein master for replica moulding vart utvikla. Ein jevn film-tjukkelse av fotoresist vart oppnådd, men det oppsto eit gjentakande problem med formasjon av ein edge bead og sprekker i resist-filmen som eit resultat av temperatur-indusert stress. Replica moulding vart brukt til å produsere PDMS-stempel frå masteren. AFM-analyse viste uregelmessigheiter i stempelet som korresponderte med sprekkane som vart observert i resisten, noko som resulterte i dårleg kontakt mellom stempelet og substrat-overflata. Parameterane for replica moulding vart verifisert ved å bruke ein forhandslaga master frå eit tidlegare prosjekt ved NTNU for å produsere stempel. Dette viste at prosessen var passande for å lage PDMS-stempel med strukturer i mikrometer-skala. Desse stempla vart brukt til å demonstrere at PDMS-stempel kunne verte brukt til å stemple PLL i mikromettermønster.

Det vart også demonstrert at *S. cerevisiae* kunne bli immobilisert på ei glassoverflate funksjonalisert med PLL.



## Acknowledgments

I want to thank my supervisor Marit Sletmoen for all the advice and support I have received during the work on my thesis.

A thanks also goes out to Aurora Ressel, Lilli Bay, Kertu Liis Krigul and Retina Shresta for the collaboration. Your help has been invaluable and your company has made the lab a much nicer place to be this year. A special thanks also goes to Nina Bjørk Arnfinnsdottir for all the startup-help and your patience in answering all of my questions. You have prevented me from making many mistakes, and for that I am extremely grateful.

I also want to thank the NTNU Nanolab staff for all the good advice when I started working in the cleanroom. I especially want to thank Mark Chiappa for all the help I have received with my lithography work and Mathilde Barriet for guiding me through my PDMS work.

Thank you to my parents for their constant support and encouragement and to my friends for keeping my spirits up through the work with my thesis.



# Table of contents

TABLE OF CONTENTS .....	VII
LIST OF FIGURES .....	VIII
<b>1. INTRODUCTION.....</b>	<b>1</b>
<b>2. BACKGROUND.....</b>	<b>2</b>
<b>3. THEORY .....</b>	<b>4</b>
3.1. SOFT LITHOGRAPHY .....	4
3.1.1. <i>Replica moulding</i> .....	5
3.1.2. <i>Elastomers</i> .....	5
3.1.3. $\mu$ CP.....	7
3.2. PHOTOLITHOGRAPHY .....	9
3.2.1. <i>Spin coating</i> .....	9
3.2.2. <i>Thermal curing</i> .....	11
3.2.3. <i>Exposure</i> .....	12
3.2.4. <i>Development</i> .....	13
3.2.5. <i>SU-8</i> .....	14
3.3. CELLULAR ADHESION .....	16
3.3.1. <i>Saccharomyces cerevisiae</i> .....	16
3.3.2. <i>Poly-L-lysine</i> .....	17
3.4. MICROSCOPY .....	18
3.4.1. <i>Light microscopy</i> .....	18
3.4.2. <i>Phase contrast microscopy</i> .....	19
3.4.3. <i>Atomic force microscopy</i> .....	20
<b>4. MATERIALS AND METHODS.....</b>	<b>22</b>
4.1. MASK DESIGN .....	22
4.2. PHOTOLITHOGRAPHY .....	22
4.3. REPLICA MOULDING .....	24
4.4. STAMP CHARACTERIZATION .....	25
4.5. MICROCONTACT PRINTING .....	<b>FEIL! BOKMERKE ER IKKE DEFINERT.</b>
4.6. YEAST CELL INOCULATION AND PROCESSING .....	26
<b>5. RESULTS AND DISCUSSION.....</b>	<b>27</b>
5.1. STARTING POINT: .....	27
5.2. METHOD OVERVIEW: .....	27
5.3. PHOTOLITHOGRAPHY OPTIMIZATION.....	29
5.3.1. <i>Process optimization for SU-8 2003.5</i> .....	29
5.3.2. <i>Process optimization for SU-8 5</i> .....	31
5.3.3. <i>Remaining challenges</i> .....	35
5.4. REPLICA MOULDING .....	38
5.4.1. <i>Stamps made from own master moulds</i> .....	39
5.4.2. <i>Remaining challenges</i> .....	42
5.5. MICROCONTACT PRINTING .....	43
5.5.1. <i>Remaining challenges</i> .....	47
5.6. AFM ANALYSIS OF STAMP SURFACE.....	48
5.6.1. <i>Immobilization of S. cerevisiae (unsure about whether to include this part)</i> .....	54
<b>6. CONCLUSION AND OUTLOOK.....</b>	<b>56</b>
<b>7. BIBLIOGRAPHY .....</b>	<b>59</b>

## List of figures

Figure 3.1-1. Chemical structure of a unit of poly(dimethyl)siloxane (PDMS). .....	6
Figure 3.2-1. Common artefacts that can occur during spin coating of photoresist. ....	10
Figure 3.2-2. Different contact modes for exposure of substrate in a mask aligner. ....	12
Figure 3.2-3. SU-8 monomer structure. ....	14
Figure 3.2-4. Photoresist film thickness of selected resists in the SU-8 series at various spin speeds. ....	15
Figure 3.3.4-1. Phase contrast microscopy working principle. ....	19
Figure 3.3.4-2. Working principle of the atom force microscope. ....	21
Figure 4.2-1. Overview of the microcontact printing procedure for cell immobilization. ....	24
Figure 5.3-1. Silicone wafers with SU-8 2003.5 covered in residue formed after development in MrDEV-600. ....	30
Figure 5.3-2. Tidemark of dried photoresist on 4” wafer with SU-8 5 photoresist. ....	32
Figure 5.3-3. SU-8 5 photoresist (3.8 $\mu\text{m}$ film thickness) exposed at 120 $\text{mJ}/\text{cm}^2$ . ....	33
Figure 5.3-4. SU-8 5 photoresist (3.8 $\mu\text{m}$ film thickness) exposed at different exposure doses. ....	34
Figure 5.3-5. Resist residues on the developed wafer after circular agitation. ....	35
Figure 5.3-6. The effect of edge bead on hard contact exposure. ....	36
Figure 5.4-1. PDMS stamp with SU-8 2003.5 photoresist residue on the stamp surface. ....	38
Figure 5.4-2. PDMS stamps with irregularities on the surface. ....	39
Figure 5.4-3. PDMS stamps produced with optimized photolithography procedure with (a) stripe and (b) square pattern. ....	40
Figure 5.4-4. PDMS stamp with a pattern of circles with decreasing size (4.4 – 0.8 $\mu\text{m}$ ). ....	41
Figure 5.5-1. Microcontact printing of PLL-FITC on glass substrates (a) with and (b) without applied weight. ....	44
Figure 5.5-2. Partial stamping of PLL-FITC after $\mu\text{CP}$ . ....	45
Figure 5.5-3. Comparison of non-plasma treated (a) and plasma treated (b) PDMS stamp for $\mu\text{CP}$ of PLL-FITC. ....	46
Figure 5.6-1. AFM height map of PDMS stamp surface. ....	48
Figure 5.6-2. Height (nm) and separation ( $\mu\text{m}$ ) of features on PDMS stamp surface. ....	49
Figure 5.6-3. AFM height map of PDMS stamp surface. ....	50
Figure 5.6-4. Height (nm) and separation ( $\mu\text{m}$ ) of features on PDMS stamp surface. ....	50
Figure 5.6-5. AFM height map of 6x6 $\mu\text{m}$ squares patterned PDMS stamp. ....	51

Figure 5.6-6. Height (nm) and vertical distance ( $\mu\text{m}$ ) between features on a PDMS stamp. . .	52
Figure 5.6-7. AFM height map of $6 \times 6 \mu\text{m}$ squares patterned PDMS stamp. ....	52
Figure 5.6-8. Height (nm) and vertical distance ( $\mu\text{m}$ ) between features on a PDMS stamp. . .	53
Figure 5.6-9. <i>S. Cerevisiae</i> immobilized on a glass surface functionalized with PLL (0.01%). .....	54

## List of tables

Table 1-1. Photoresists and optimized spin parameters for photolithography. ....	23
Table 5-1. Spin parameters and achieved film thickness for SU-8 2003-5 photoresist. ....	29
Table 5-2. Spin speed and film thickness for SU-8 5 photoresist on 4" silicon wafers. ....	31

## Abbreviations

AFM	Atom force microscope
DI	De-ionized
$\mu\text{CP}$	Microcontact printing
MOPS	3-(N-morpholino)propanesulfonic acid
MQ	MilliQ
PDMS	Poly(dimethyl)siloxane
PEB	Post exposure bake
PLL	Poly-L-lysine
SCA	Single cell analysis
YPD	Yeast extract peptone dextrose



# 1. Introduction

Humans have been studying single cells since the 1600s when Van Leuwenhoek first managed to make cells visible in his single lens microscope (1). Since the discovery of cells, biology has undergone several revolutionary changes of understanding. Deducing the structure of DNA led to the beginning of the era of –omics in molecular biology and systems biology (2). DNA sequencing and analysis has developed at an increasing rate and has given rise to the field of genomics. Proteomics, transcriptomics and metabolomics have followed. Technological developments have enabled biologists to access unprecedented amounts of data. The development of the field of systems biology tools enabled processing the data and allowed high throughput analysis (3).

The investigation of populations of cells today, including their heterogeneity, is still largely based on bulk measurements, but there is an increasing interest in achieving high throughput platforms for single cell analysis (SCA) (4). However, this entails a need to develop platforms for cheap, reproducible SCA methods (5). There is also interest in tracking single cells over time and use AFM for cell surface studies. AFM studies require immobilization to prevent the stylus from pushing the cells across the surface (6, 7).

Microcontact printing is a soft lithography method for surface functionalization that enables micro- and nanoscale patterning (8). A patterned elastomer stamp can be used to transfer a cell-binding chemical to a substrate surface (5, 9). This offers a cheap and reproducible method for patterning large surfaces (10).

Goals of the thesis:

- Produce PDMS stamps with micrometre features
- Develop a method for characterizing stamp surfaces
- Deposit PLL in a pattern using microcontact printing
- Immobilize *Saccharomyces cerevisiae* on the PLL pattern

## 2. Background

Cellular heterogeneity within a population is a well-known phenomenon in bacterial cell populations where bacteria that have developed from the same mother cell and in similar growth conditions still exhibit different phenotypes (4, 11). A possible cause of the variation is random mutations, but it can also result from stochastic variation in gene expression (2). The phenomenon is also becoming increasingly recognized in eukaryotic cells. Cellular heterogeneity is an important factor in the lethality of human cancers as it contributes to the ability of cancer cells to survive chemotherapy and radiation treatment (12). It is also being recognized as an important factor in antibiotic resistance, which is steadily becoming a larger threat to human health in worldwide perspective due to the overuse of antibiotic treatment (13).

Cellular heterogeneity is a fundamental property of biology and causes phenotypic variation between cells containing the same DNA (2). Arising from factors such as mutations, genetic drift, cell age or cell cycle status or non-genetic variation from stochastic gene expression, this heterogeneity can have an important influence on cell fate and development (3). Standard molecular biology techniques rely on bulk measurements that provide average values for any of the measured parameters (14). The measurements work under the assumption that this information will be true for each of the individual cells. While this is often a very useful simplification, it can also give misleading information about the state of the cell population (3). An example is the study by the Mathies group of GADPH gene expression in Jurkat cells after siRNA knockout treatment. Average results from 50 cells gave a gene expression of 21%. However, single cell analysis using a microfluidic bioprocessor revealed two distinct groups of cells with either 50 % or 0% GADPH expression. The average values did not give an accurate picture of either group (15).

Single cell analysis has been achieved by the use of several different techniques, but there are several challenges associated with achieving high throughput platforms (2). A well-established and powerful method for single cell analysis is microscopic analysis, which is mainly being used for morphological studies, gene and protein expression and intracellular communication. It is a generic method that is easily accessible for molecular biology laboratories, but is limited in the possibility for single cell assays. Patch clamp studies have been used specifically for ion channel studied, but require a high level of skill to be used and

cannot be transferred to a high throughput platform. Optical and magnetic tweezers are also used for SCA, mainly for manipulation and the study of single cell mechanics. Another common SCA method is flow cytometry, which can easily be adapted for high throughput analysis. Fluorescence assisted sorting cytometry (FACS) can be utilized to separate different types of cells in a sample. The major drawback of using flow cytometry is that data is only collected at one specific time point, making dynamic monitoring of cells impossible (3).

Nanobiotechnology approaches open up new possibilities for high throughput platforms for SCA. The use of microfluidic approaches permits a wide range of applications and is a potential high throughput platform for single cell analysis. Microfluidic platforms have been coupled to microscopy and has extensive used in drug development (16). However, it requires the use of specialized equipment that is not necessarily available to a standard molecular biology lab and has not yet been established as a common method (5). Patterning of surfaces to facilitate cell adhesion has also been utilized to enable SCA. The basic principle behind the patterning approach is to create surface patches onto which cells are likely to attach contrasted by cell-repellent areas on the substrate surface (17). Microcontact printing uses an elastomeric material with designed features to create a precise pattern on the substrate surface. This enables a precise control over cell location on the surface down to a micro- or nanometer scale, so that high throughput analysis of the attached cells becomes feasible (18).

## 3. Theory

### 3.1. Soft lithography

Microfabrication has become an essential feature of many fields of modern technology, most obviously in microelectronics where it has enabled the production of chips that are smaller, less expensive, with more components per chip, faster operation, higher performance and lower power consumption. Miniaturization has opened up many new possibilities by allowing for integration of a range of devices that has enabled portability, smaller sample sizes and higher throughput (5).

Recent years have seen the development of the field of nanobiotechnology, which combines nanotechnology and microfabrication methods with molecular biology techniques. On one hand, biomolecules are an example of functional nanostructures that can be useful for nanotechnology and has had a strong influence on the development of bottom-up fabrication techniques and the use of self-assembly. On the other hand, micro- and nano-devices can be very useful when studying biological processes. Biofunctionalization of surfaces and microfluidic devices have both developed into high throughput methods for cell analysis. Techniques like photolithography, electron- and focused-ion-beam and X-ray lithographies, together with scanning probe methods have become well-established high-throughput methods in the field of nanotechnology, but they generally lack biocompatibility and are in many ways inaccessible to molecular biologists, as they require access to cleanroom facilities or highly specific equipment. There is also a high cost associated with most of the techniques (8).

Soft lithography techniques provide alternative approaches for microfabrication. The techniques referred to as important soft lithography techniques are microcontact printing ( $\mu$ CP), replica moulding, microtransfer moulding ( $\mu$ TM), micromoulding in capillaries and solvent-assisted micromoulding. These techniques are collectively referred to as soft lithography due to the use of an elastomer stamp and flexible organic molecules to transfer a pattern to the substrate. This contrasts the rigid inorganic materials commonly used in fabrication of microelectronics. Soft lithography generates micropatterns of self-assembled monolayers by contact printing and in materials by embossing. A strength of soft lithography is in the replication of the master, rather than its fabrication. Rapid prototyping and the ability to deform the elastomeric stamp or mould provide unique capabilities even in fabricating

master patterns. Soft lithographic techniques are cheaper and procedurally simpler than standard photolithography. A large advantage is that they can often be carried out in the ambient laboratory environment. They are also not subjected to the limitations set by optical diffraction and optical transparency that apply in photolithography. The edge definition is set by van der Waals interactions and the properties of the materials involved (5).

### **3.1.1. Replica moulding**

The enabling technique in soft lithography is replica moulding, the generation of an elastomeric replica of a master mould. The master mould, which contains micro-or nanoscale topography, is covered in the elastomer pre-polymer in a liquid state. *In situ* polymerization is then performed, most commonly through thermal curing. After curing, the replica can be peeled away from the master by slightly reversible deformation (19). The elastic quality of the polymer enables the replication of the master and the possibility of repeating this process hundreds of times without introducing damage to the structure of the master regardless of the complexity. It also allows the creation of a 3D structure in a single step. The technique of replica moulding is cheaper than all other comparable technologies and has the added advantage of being possible to perform in ambient laboratory conditions without the need for cleanroom facilities. These two characteristics makes replica moulding a very suitable method for biologists that can be used in their standard laboratories (20). As a large number of replicas can be formed from a single master with little additional cost for each replica, the cost of producing the master can be spread out over many samples. This enables the use of high-resolution advanced lithography like photolithography or EBL to create the master mould, as the many replicates produced will justify this single high cost. Replica moulding demonstrates that soft nanotechnology can replicate the information provided by the structure of a master mould (9).

### **3.1.2. Elastomers**

Elastomers are polymers with elastic properties and low surface energies, making them suitable for transferring molecules onto a surface. Poly(dimethyl)siloxane is the primary elastomer used in soft lithography (20).

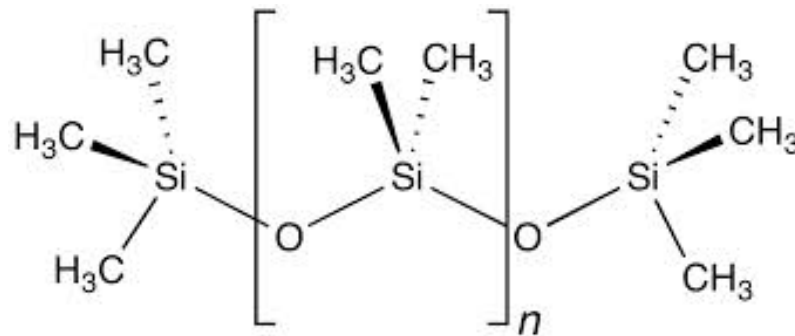


**Figure 3.1-1. Chemical structure of a unit of poly(dimethyl)siloxane (PDMS).**

PDMS is a linear polymer consisting of a Si-O backbone and with two methyl side groups on each Si atom. Several physical and chemical characteristics of PDMS make it suitable for work with biological material: it is chemically inert, compatible with optical detection (transparent for wavelengths 300-800 nm), non-toxic to cells and proteins and gas-permeable. In addition, it is stable at all temperatures where biological reactions usually occur (40-95 °C) (9). Commercially available PDMS, such as Sylgard 184 from Dow Corning, commonly consists of a pre-polymer base and a curing agent. It exists in a liquid state at room temperature and is typically solidified through thermal curing. Curing times and temperatures vary and different parameters are preferred depending on the structures used (21). PDMS has a low Young's modulus value of around 3 MPa, which guarantees the mechanical stability of the elastomeric features. However, there is also a risk of loss of resolution because the moulds can suffer distortions, collapse or sagging (8). To increase the usefulness of PDMS, new variations have been introduced in later years. For sub-micrometre features, hard PDMS (h-PDMS) has been suggested. In h-PDMS, siloxanes with vinyl and hydride groups are blended and cross-linked through a hydrosilylation reaction (22).

Surface characteristics of the elastomers are extremely important to their functionality in soft lithography. A specific property of PDMS is the low surface energy of around 22 nM/m and the strong hydrophobicity with a water contact angle of around 110°. This means that small hydrophobic molecules, biopolymers and cells can adhere temporarily to the PDMS surface, but that aqueous solutions are unable to bind (8). Several techniques have been developed to alter the characteristics of PDMS either reversibly or permanently. Plasma oxygen treatment has been shown to create transient silanol functional groups on the PDMS surface. These groups can then be used as reactive sites for bonding of organic groups. Other techniques that have been used for the same purpose include exposure to UV, UV/ozone irradiation,

photograft polymerization and attachment of hydrophobic molecules to the PDMS surface (5).

Another unique advantage of PDMS over glass, silicone and hard plastics is the ability to be bonded to different substrates in a reversible or irreversible way. PDMS bonding can be achieved with temperatures in the range of 600 – 1000 °C or anodic bonding with voltages up to 500 V, which is much lower than what is required for many other substrates (8). In addition to the relatively easy bonding, PDMS can also be sealed to substances such as glass, silicone, polystyrene and polyethylene to create hybrid devices such as the devices used for microfluidics. The reversible sealing process is mediated by van der Waals forces, which allow the PDMS to provide conformal contact with other surfaces (23). Irreversible sealing is achieved in a couple of different ways depending on the type of substrate one is working with, but the most common method is oxygen plasma treatment of both PDMS and substrate. This treatment induces formation of silanol groups on the PDMS and –OH-groups on the substrate surface so that covalent O-Si-O-bonds form when the two are brought into contact. Two PDMS stamps can also be sealed to each other using a thermal approach (18).

### **3.1.3. $\mu$ CP**

Contact printing is a method of pattern transfer with high efficiency. Conformal contact between the stamp and the substrate is the determining process for the success of the printing process. Printing is a simple and convenient method, once the stamp is available, multiple copies of the pattern can be produced from the stamp through simple experimental methods (19). It is an additive method with minimal waste of materials and also has the potential to be used for patterning larger surfaces. This method is most suitable for the creation of 2D patterned surfaces, but with some potential of creating simple 3D structures when combined with other methods (10).

Microcontact printing ( $\mu$ CP) is a non-photolithographic method that is used to pattern molecules of different chemical functionalities in a substrate with a resolution on the micrometre scale. An elastomeric stamp is used to transfer molecules of an “ink” solution to the surface of the substrate by contact. This is a quick process and ink can be transferred after only a few seconds of contact, depending on the type of solution used (10). After printing, a different chemical can be formed by backfilling the un-derivatised regions. The pattern formed by  $\mu$ CP can be visualized using methods such as SEM, scanning probe microscopy or

simply printing a fluorescently dyed chemical and using fluorescence microscopy.  $\mu$ CP is attractive due to being flexible, simple and inexpensive. When a mould has been created, the microcontact printing itself does not require access to cleanroom facilities and can be performed in a standard biology lab at low cost. A particular strength compared to photolithography is the ability to pattern non-planar surfaces. It can also efficiently be used to pattern larger areas in one printing step (24).

$\mu$ CP has been developed for use with patterning of proteins and DNA and to control spatial distribution of cells on a solid support. The technique has been shown to be particularly useful for immobilization of proteins in spatially controlled areas on a substrate. The principle behind  $\mu$ CP is the transfer of molecules onto a substrate surface through the contact between the raised features of the stamp, coated with a solution containing molecules, and the substrate surface (20). The process consists of some fairly simple steps. A stamp produced through replica moulding is coated with a solution of the molecule to be stamped, referred to as the “ink”. The excess solution is removed through evaporation and the replica is placed in conformal contact with a substrate surface such as a glass slide or a Petri dish. When peeling off the stamp, the stamped molecules remain on the substrate (25). The adhesion to the substrate can be non-specific or specific. An example of non-specific interactions is the attachment of charged molecules to glass slides through electrostatic interactions. A common specific interaction that is utilized for adhesion is the binding between streptavidin and a molecule containing a biotin group, which is the strongest known interaction in biology. As only the raised areas of the elastomer come into contact with the substrate surface, there is a high degree of control in where the ink is transferred. This results in an ordered, patterned surface (18).

There has been some concern that the stamping process could cause deformation and loss of function of some biomolecules. The drying process and interaction with the substrate surface could potentially influence aggregation and functionality (24). Studies do however show that protein functionality is retained in most cases. Performing the procedure at room temperature and using solvents compatible with the inked molecule can preserve the functionality. The use of immune-fluorescence assays has confirmed that structure and function of proteins is intact after stamping.  $\mu$ CP can easily be combined with standard biology detection methods, particularly fluorescence microscopy. The stamped molecules can be tagged with a

fluorescent molecule to provide a simple and efficient strategy for characterization and quality control of the stamped surfaces (18).

### **3.2. Photolithography**

Photolithography is an optical means for transferring patterns from a photomask onto a substrate. The pattern is first transferred onto a photoresist layer that is coated on a surface such as a silicone wafer or a glass slide. The photoresist is a photosensitive chemical that reacts to exposure to UV light. They are grouped in two main groups depending on their reaction to UV-exposure: negative and positive tone resists. Negative photoresists form cross-links when exposed to UV-light, whereas non-exposed areas can be removed in developer solution. Use of these resists produce a negative of the image on the photomask. A positive photoresist cross-links when not exposed to light, whereas exposed areas can be removed in developer solution (26). This produces an identical copy of the pattern on the photomask. The photomask is a structure that blocks UV-light in some areas and contains the pattern to be transferred. It can be made from printed chromium or more simple polymer films that have a shorter lifetime. Printed chromium masks have a higher resolution and enable the production of smaller pattern structures. The substrate used can be glass, but is most commonly a silicone wafer that is coated with a layer of photoresist (5).

#### **3.2.1. Spin coating**

Spin coating is the most common method for applying photoresist to the substrate. Alternative approaches include spray coating, dip coating and roller coating. Due to achieved homogeneity of the resist combined with a short coating time, spin coating is generally preferred. It works by using centrifugal forces to spread a few ml of photoresist across the substrate surface while spinning at 1000 rpm or higher (27). There are four distinct phases of the spin coating process: deposition, spin-up, spin-off and evaporation of the solvent. Deposition, spin-up and spin-off occur sequentially, but spin-off and evaporation often overlap. The last two stages are most important for determining the final resist film thickness.

Thickness of the resist film is given by the equation  $t \propto \frac{1}{\sqrt{\omega}}$  where  $t$  is the film thickness and  $\omega$  is the angular velocity (28). There are many advantages to using this coating method. It has no coupled variables, film thickness is easily modified through changing spin speed or resist viscosity and the method is versatile. The process is quick. However, there is a significant

drawback of low material efficiency (29). Up to 95-98 % of the applied photoresist is flung into the bowl of the spin coater and thus disposed. The high cost of photoresist and chemical waste disposal makes this a disadvantage. It is also difficult to make thin coats on large substrates (28).

Resist layers from 1  $\mu\text{m}$  to more than 200  $\mu\text{m}$  are possible, although the most common uses are 25-80  $\mu\text{m}$ . Thickness also depends on the solvent concentration of the resist, which changes during spinning. The concentration saturates at around 15-25 % solvents, depending on the thickness of the film. A thicker film layer will generally retain a larger amount of solvent after the spin process (27).

Optimization of the spin parameters is important to achieve a homogenous layer of photoresist. Several possible artefacts may occur during spin coating if it is not performed properly (figure 3.2-1).

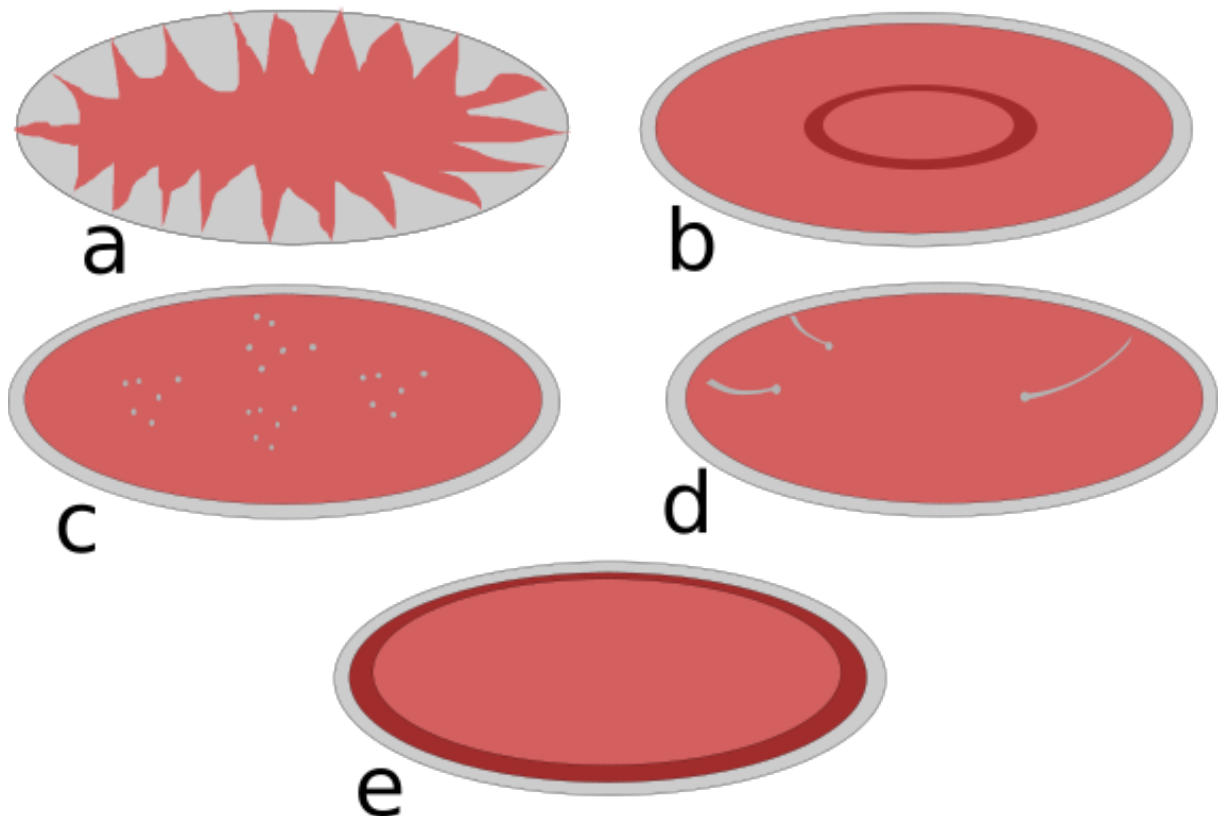


**Figure 3.2-1. Common artefacts that can occur during spin coating of photoresist. (a) Uncoated areas of the substrate, (b) a tidemark, (c) pinholes, (d) comets/streaks and (e) edge bead.**

Uncoated areas of the wafer can be a result of too high spin speed in the initial phase or application of an insufficient amount of resist. A common approximation is to use 1 ml of

photoresist for each inch of wafer surface to get sufficient coverage (30). Tidemarks refer to a dried area of resist that occurs around the area where the resist is applied prior to spinning. This can cause a circle of thicker resist film in the middle of the wafer. Pinholes and comets are holes in the resist layer that are usually a result of particle contamination on the substrate or in the resist, which can be resolved through a more thorough cleaning process and proper cleanroom method. Another possible cause is the presence of air bubbles in the resist (27). The presence of an edge bead is frequent, especially when working with thicker layers of resist ( $>100\ \mu\text{m}$ ). The edge bead is an area on the outer edge of the substrate where the film is thicker than the rest of the layer. This can interfere with the exposure, as the thicker areas of film will reflect the light in unpredictable ways and reduce lateral resolution (27). If hard contact exposure is used, the edge bead can also contaminate the mask. An edge bead can be avoided by adding a spin-off step to the end of the spin with a slightly higher spin speed. It can also be removed by cleaning the outer edge of the wafer with a solvent. The removal can be performed automatically in some spinners by applying solvent to the substrate edge with a small needle during spinning, but it can also be performed manually (27).

### **3.2.2. Thermal curing**

Thermal curing solidifies photoresist through further solvent evaporation, giving a final solvent concentration of approximately 5% (26). The substrate can be cured in an oven or on a hot plate. A hot plate is generally preferred because it gives a more even bake of the resist film. Using an oven is also more time consuming as there is no direct contact between the substrate and the heat source (31). Thermal curing of the resist is performed in two or three separate steps throughout the photolithography process: soft bake, post-exposure bake (PEB) and hard bake. The soft bake is performed directly after spinning on the resist and makes the resist go solid on the substrate. Most resists also require a PEB after exposure to UV-light. During PEB, the resist forms crosslinks in the areas that were exposed to light (for a negative tone photoresist), making the pattern stable in the developer solution. Both the soft bake and the PEB are performed by gradually increasing the temperature to the desired end temperature to reduce the amount of thermal stress applied to the photoresist (32).

Some photoresists such as SU-8 are prone to thermal stress, especially when using thicker resist films (33). Thermal stress can result in formation of cracks in the resist, which disrupts the pattern and disrupts replica moulding because the uncured pre-polymer will go into the

cracks and create heightened structures outside of the pattern. The PEB temperature has been suggested as the most important factor for inducing thermal stress in SU-8 photoresist (32). Another important factor is the rate of cool-down after the bake. A too rapid decrease in temperature, for example the use of a cooling block, can cause cracks in the resist. The resist should therefore be cooled gradually down to room temperature (32). If the photoresist is going to be a part of the finished device and will be exposed to high temperatures, a hard bake can also be included in the process. The hard bake is performed after development to increase resist stability further (29).

### 3.2.3. Exposure

A typical mask aligner has a Hg lamp as the light source and contains g-, h- and i-line with wavelengths of 436 nm, 405 nm and 365 nm respectively. The i-line intensity is approximately 40 % of the total emission from 440 to 340 nm. Most unexposed photoresists have an optical absorption range from 440 nm (VIS) to near UV light. This absorption range is matched to the emission spectrum of Hg lamps. SU-8 resist is most commonly exposed with regular near UV light characterised by wavelengths in the range 350-400 nm. The best results are achieved using i-line (365 nm), but a beam of electrons or x-rays can also be used (34).

Prior to exposure, the substrate is aligned with the photomask and brought into proximity in one of several possible ways. A lower exposure gap between mask and wafer gives a higher resolution. A cheap method for producing structures down to 3  $\mu\text{m}$  in size is the use of proximity lithography where the substrate is brought into proximity to the mask before exposure without touching the mask. The method is fast and cost effective, but cannot be used to create structures in the sub-micrometre range (35). Nanometre features require the use of contact exposure. Contact between the substrate and the mask can be established as soft contact, hard contact or vacuum contact exposure (figure 3.2-2) (36).

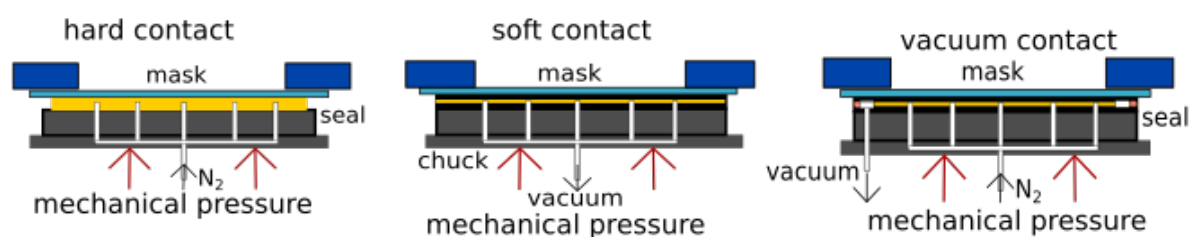


**Figure 3.2-2. Different contact modes for exposure of substrate in a mask aligner.**

In hard contact, the wafer is brought into direct contact with the mask. The contact is maintained through mechanical pressure from applied nitrogen gas. Hard contact enables making features down to a 1 $\mu\text{m}$  size. With soft contact, vacuum is applied to fix the mask on the chuck and the wafer is brought into contact with the mask. This increases the resolution compared to hard contact exposure. With vacuum contact exposure, the substrate is sealed to the mask with vacuum and achieves a resolution of  $< 0.8 \mu\text{m}$  (36).

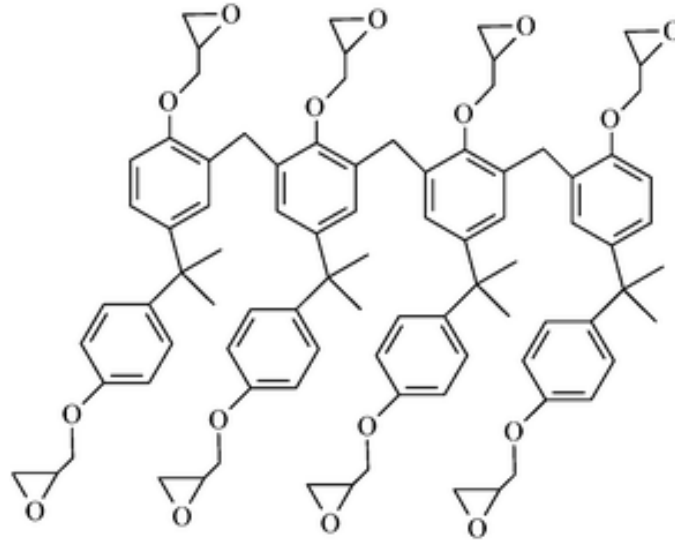
The exposure dose needs to be optimized for each specific procedure. The optimum exposure dose for positive resist is achieved when the development rate starts to saturate. An under-exposed substrate will have increased development time and also increased dark erosion. An over-exposed subject will experience light scattering and diffraction in the resist film, which decreases the resolution (27). Negative resists contain a cross-linker that is activated during exposure and is thermally induced to crosslink resins during the post exposure bake. Increasing the exposure dose leads to a higher degree of cross-linking, improved thermal and chemical stability and also influences the resist profile after development. Generally, when developing a new procedure, an exposure series varying from around 50 % to 200 % of the estimated optimum dose is found to be required to determine the correct exposure (34). Both over and under exposure cause reduced quality of the resist film. For insufficient exposure doses, the light is unable to penetrate the entire resist film and if the dose is very low the pattern could not be transferred at all. For too high exposure, light will also be diffracted under the areas blocked by the pattern of the mask (34).

#### **3.2.4. Development**

Photoresist developers are generally either alkaline-based solutions (TMAH or NaOH-based) or solvent-based solutions. An example of a solvent-based developer is the mrDev-600 developer for the SU-8 resists series. A substrate is developed either by spraying the surface with developer or fully submerging it in a beaker of the solution (26). Development time increases with increasing film thickness and is also dependent on exposure dose and thermal curing time. Increasing the temperature of the developer can be used to reduce the time needed for development. The development time needs to be adjusted based on the total photolithography process (26).

### 3.2.5. SU-8

SU-8 is a negative-tone photoresist from Microchemicals. It is an epoxy-based resist that consists of an epoxy dissolved in the organic solvent cyclopentanone and a photoacid generator (37). Older versions of the resist used GBA as the solvent, but changing to cyclopentanone improved performance. The resist also contains a salt that acts as the photoacid generator. SU-8 is a monomer (figure 3.2-3) that forms crosslinks during the photolithography process (37).



**Figur 3.2-3. SU-8 monomer structure. Figure from (38).**

Cross-linking of the resist occurs through two separate steps. A strong acid is formed during the exposure process followed by an acid-initiated, thermally driven epoxy cross-linking during the PEB step (37).

Different film thicknesses can be achieved using SU-8, depending on the solid content (amount of epoxy that is dissolved) and the spin parameters applied when coating the substrate (Figure 3.2-4) (33).

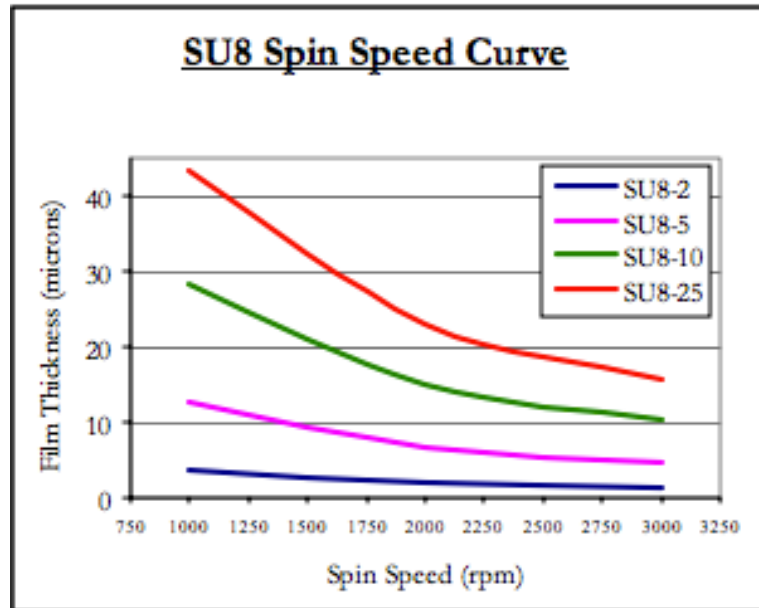


**Figure 3.2-4. Photoresist film thickness of selected resists in the SU-8 series at various spin speeds.** Figure from (30).

SU-8 is highly suitable for replica moulding applications and microfluidic devices due to the high aspect ratio that can be achieved (32). The resist has high thermal stability and can be used as part of the final device. Film thicknesses down to 2  $\mu\text{m}$  can be achieved using more diluted versions of SU-8 with a lower solid content (30).

### **3.3. Cellular adhesion**

#### **3.3.1. *Saccharomyces cerevisiae***

The yeast *Saccharomyces cerevisiae* is a unicellular fungus in the *Saccharomycetaceae* family, which has been utilized by humans for hundreds of years. *Saccharomyces cerevisiae* can exist in either a diploid or a haploid state because the organism is capable of both asexual and sexual reproduction. Asexual reproduction occurs by budding where the daughter cells separates from the mother cell through mitotic cell division. Both cells will have a budding scar formed at the cell wall surface at the point of separation. This can be observed under a microscope (39). Sexual reproduction occurs when two yeast cells of opposite mating types fuse and divide to form four daughter cells. Original uses of the organism were in brewing and baking, which are still important uses of *S. cerevisiae* today. During the development of modern biotechnology, the yeast became a eukaryotic model organism that is extensively used in research. In 1994, it became the first eukaryotic organism to have its entire genome sequenced (40). Current uses of *S. cerevisiae* also include the industrial production of low-value/high volume chemicals like bioethanol and high-value/low volume chemicals like artemisinin (7).

During industrial scale production of biochemicals, the cells are exposed to a variety of environmental stress factors including changes in pH, temperature and cell density. Biochemical and molecular techniques have enabled scientists to demonstrate that cells are able to react to environmental signals through plasma membrane cell sensors that start a signal transduction cascade triggering an intracellular response (41). Building on these results, there is an interest in visualizing and quantifying these stress responses. Especially interesting would be visualizing the events on the cell surface to determine how the cell wall is affected by different stresses. Proteins in the cell wall play crucial roles in cell adhesion, cell-cell communication and pathogenic activity of the yeast cells. The activity of these proteins in response to external signals and as a part of the signal transduction machinery of the cell is still not completely understood (42). Further knowledge about this would aid understanding physiological and biotechnological processes like cell-cell recognition, adhesion, aggregation, flocculation, biofilm formation, resistance to antifungal drugs and barrier or mycotoxins compounds. The use of atomic force microscopy to study the yeast cell wall has given rise to a lot of new insight in the microscale structures of the cell wall and the importance of chitosan for elasticity (6).

### 3.3.2. Poly-L-lysine

Poly-L-lysine (PLL) is a positively charged polymer that has frequently been utilized to immobilize cells on various surfaces (43). The polymer is made up of  $\alpha$ -poly-L-lysine monomers (figure 3.4-1).

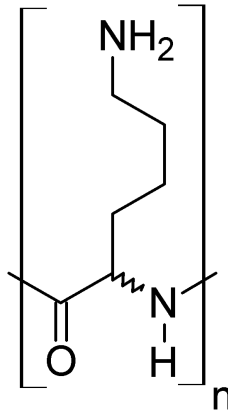


**Figure 3.4-1. Poly-L-lysine monomer. Figure from (44).**

PLL is able to bind to several different substrates, including glass, metals and metal oxides. Binding ability is influenced by the surrounding solution. Buffer facilitates PLL binding to a greater degree than deionized water. Low pH values of the solution will also negatively impact the adhesion of PLL (45). The polymer has a positive charge in acidic and neutral solutions due to protonation of the amino groups (43).

PLL immobilizes cells through a non-specific electrostatic interaction. In acidic and neutral solutions, PLL has a positive charge that can bind the negatively charged surface of cells. It has been demonstrated that PLL can have an inhibitory effect on microbial growth in sufficiently high concentrations (46). However, fungi such as yeast are more protected than animal cells due to the presence of the cell wall (47).

### **3.4. Microscopy**

#### **3.4.1. Light microscopy**

The simplest light microscope is the bright field microscope. The microscope consists of a light source, a condenser lens, an objective lens and an ocular. A halogen lamp is the common light source. Light first passes through the condenser lens, where it is focused onto a small area of the sample. The objective lens collects the light that is diffracted by the sample to create the magnified image. The oculars then magnify and view the images that have been produced by the objective (48).

Even illumination is achieved through Köhler illumination. The collector lens is used to form an image of the light source in the front aperture of the condenser. The condenser lens is used to form an image of the field stop diaphragm in the object. The condenser diaphragm is placed in the front focal plane in the condenser lens. The field stop diaphragm has a distinct area illuminated by the light source, limiting the light scattered from areas outside the sample. This contributes to the image formation. The front aperture of the condenser is located in the focal plane of the condenser lens, ensuring that light from the same point in the light source enter the object in parallel. This ensures bright and even illumination of the sample (48).

Lateral resolution in microscopy refers to how close to objects can be before the microscope is no longer able to recognize them as two separate objects. In a light microscope, resolution is limited by the wavelength of light as well as the numerical aperture. Visible light has wavelengths ranging from 0.4 to 0.7  $\mu\text{m}$  (violet to deep red light). The numerical aperture (NA) describes the entry pupil width of the microscope. The NA value can be up to 1.4 when using oil immersion (49). The limit of resolution is given by the equation

$d = \frac{0.61 \lambda}{NA}$  where  $\lambda$  is the wavelength of light and NA is the numerical aperture (48). Using violet light and oil immersion, a resolution of 0.2  $\mu\text{m}$  can be achieved with a light microscope (49).

In addition to sufficient resolution, contrast is paramount for good imaging. In unstained biological samples, the contrast is usually very low. In brightfield microscopes, scattering and absorption of the light by the sample causes contrast. Scattered light does not contribute to the image and absorbed light causes differences in intensity. Brightfield microscopes are suitable for the study of samples that have contrast, such as samples that are naturally pigmented or

samples that have been dyed. Pigments or dyes absorb specific wavelengths and cause the objects to appear coloured when illuminated by white light. However, many biological samples are transparent and are therefore difficult to image with a brightfield light microscope. For such samples, alternative microscope setups can be utilized to increase the contrast (48).

### 3.4.2. Phase contrast microscopy

The light passing through a sample is diffracted and phase shifted. Phase shifts are not visible, but they are transferred to visible differences in intensity by the phase contrast microscope. The light is separated into background light that is un-diffracted by the sample and light that is scattered by the sample. Only a small portion of the light will be scattered. The background light and the scattered light are both collected by the objective lens and focused in the image plane. They go through different optical pathways, undergo interference to generate a particle wave (figure 3.4-1) (48).

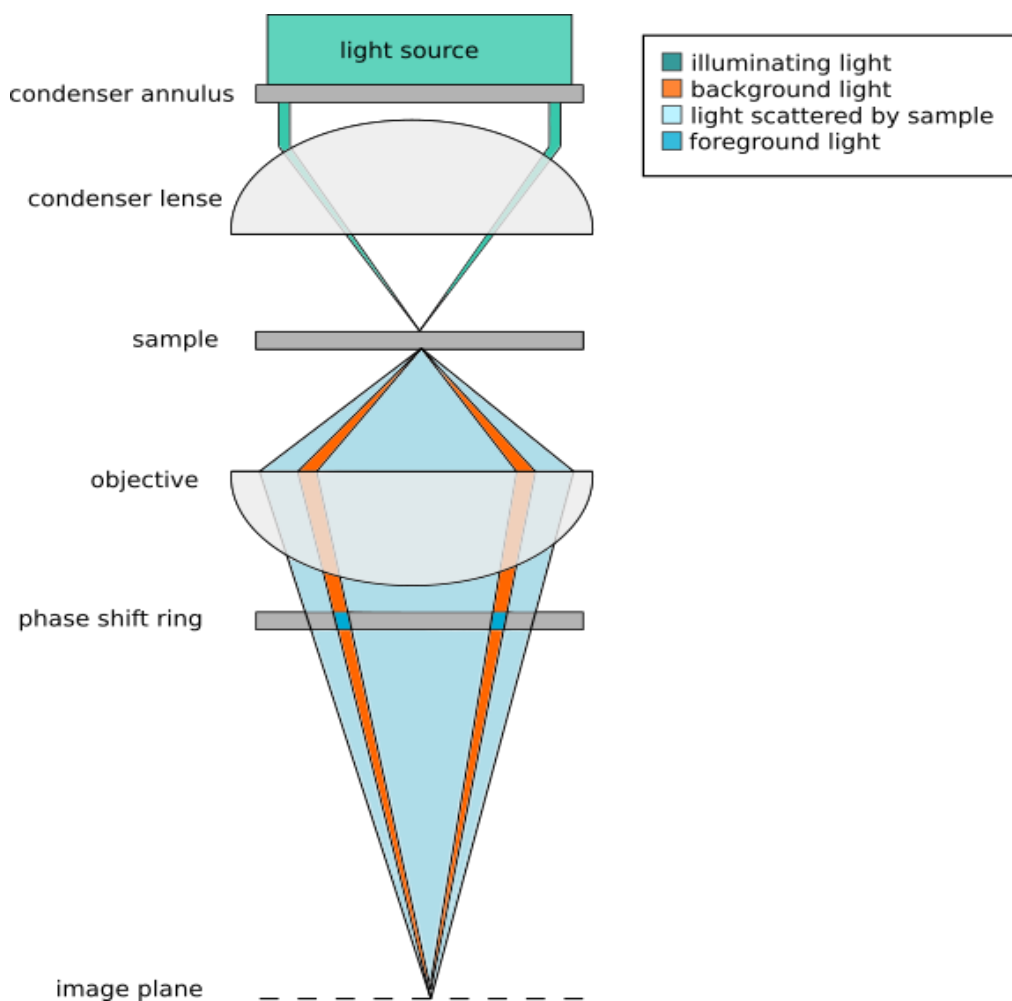


Figure 3.4-1. Phase contrast microscopy working principle.

Phase contrast microscope contains a ring-shaped aperture diaphragm and a phase plate in the back of the focal plate. The phase plate is a glass plate with a partially transparent ring. The scattered light wave is phase-shifted by  $\lambda/4$  relative to the background wave. In positive phase contrast, the background wave is advanced by  $\lambda/4$  to get a total phase shift of  $\lambda/2$ . This enables destructive interference with the scattered light wave in the image plane. Samples with higher refractive index than the medium will appear dark, while samples with lower refractive index appear light. In negative phase contrast, the background wave is retarded by  $\lambda/4$  to get a total phase shift of 0. This enables constructive interference between the scattered and background waves (48).

Phase shift in itself is not sufficient to achieve contrast because the amplitude of the background wave is too high. To solve this, the ring in the phase plate is darkened by a semi-transparent metallic coating, which reduces the amplitude of the background light wave by approximately 70 %. The particle wave that is generated has lower amplitude than the background wave due to interference in the image plane. This increases the contrast in the image. The difference in phase from diffraction by the sample has been translated to visible differences in contrast (48).

### **3.4.3. Atomic force microscopy**

Atom force microscopy (AFM) is a useful technique for enabling study of detailed structures on surfaces. A small, sharply pointed tip attached to a cantilever is used to scan the sample surface (49). A laser beam is reflected off the cantilever and detected by a photodiode. As the microscope tip is moved across the sample surface, attractive forces cause the cantilever to deflect towards the surface. When the tip gets sufficiently close, repulsive forces take over and cause the cantilever to deflect away. The photodiode measures the deflection of the reflected laser beam and uses this information to generate an image of the surface (figure 3.5-2) (49).

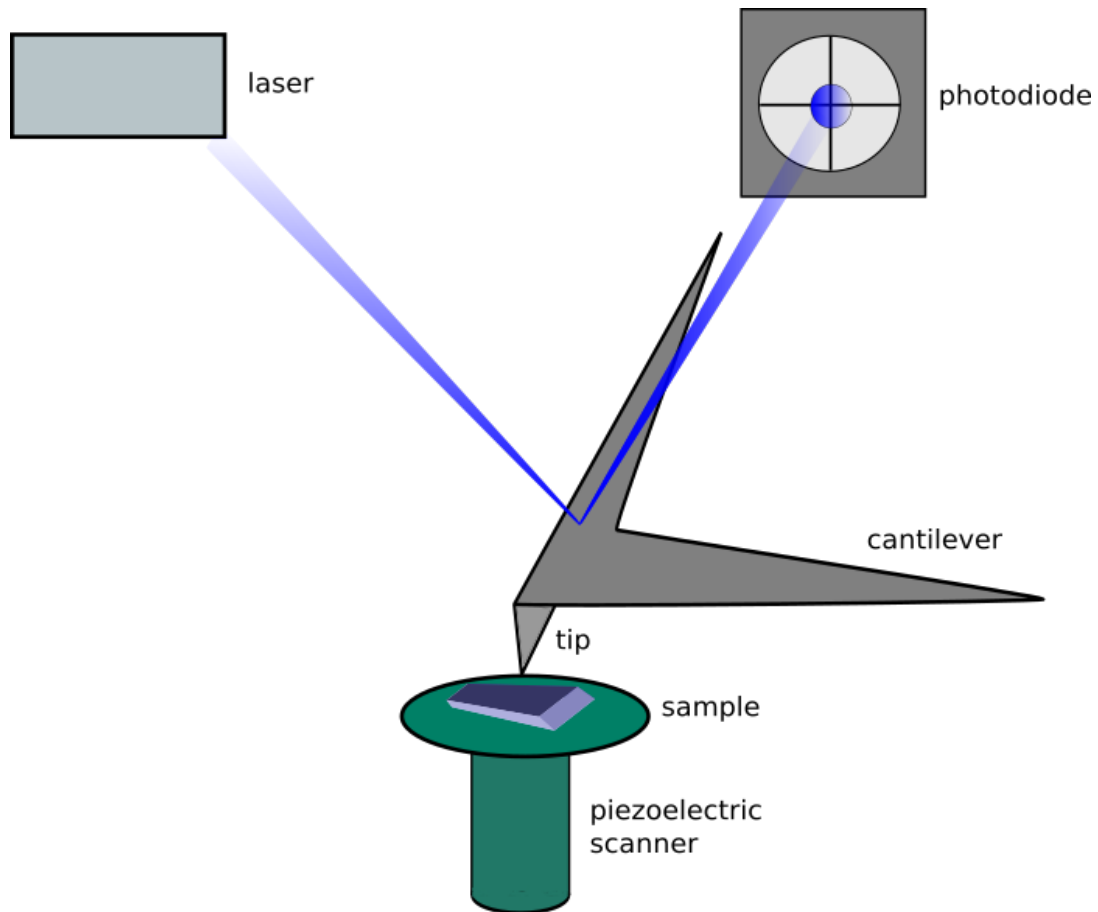


**Figure 3.3.4-2. Working principle of the atom force microscope**

The AFM can operate either in contact or oscillation mode for imaging. In contact mode, the cantilever deflection is constant, applying a constant force to the surface and generating an isoforce image. PDMS. In oscillation mode, the cantilever oscillates near resonance frequency and changes in amplitude is used to image surface topography. Oscillation mode limits damage to biological samples from contact with the AFM tip and is therefore preferred in some cases (50). AFM studies have been used to image a large variety of substrates, ranging from silicone surfaces to biological samples. It can also be used for the study of PDMS stamps (51).

In addition to imaging, the AFM is capable of sensitive force measurements of interaction between the tip and the sample surface. The AFM measures forces such as mechanical contact forces, chemical binding and van der Waals forces (48). It can be used to generate force-distance curves and has sensitivity down to 10-20 pN (50).

## 4. Materials and methods

### 4.1. Mask design

The mask used in this project was designed by Nina Björk Arnfinnsdottir and produced by Computographics. The mask used was a 5” chromium mask with four separate quadrants. One quadrant contained a pattern of stripes with thicknesses of 5, 8 and 10  $\mu\text{m}$  with a distance between the stripes equal to the width. The three other quadrants contain squares of sizes  $4\times 4\ \mu\text{m}$ ,  $6\times 6\ \mu\text{m}$  and  $8\times 8\ \mu\text{m}$  with a separation distance equal to the length of the feature sides.

### 4.2. Photolithography

4” silicone wafers (University Wafers) were coated with SU-8 2003.5 or SU-8 5 from Microchem. SU-8 2003.5 was diluted from SU-8 2100 (Microchemicals) with the SU-8 diluter cyclopentanone (Microchemicals). SU-8 2100 has an initial solid concentration of 75 %, which was diluted to a concentration of 37% to create SU-8 2003.5 with the desired viscosity. The amounts of resist and cyclopentanone required were calculated using the formula:

$$\text{Final weight} = \text{Initial weight} \times \frac{\text{Initial concentration}}{\text{Final concentration}}$$

Cyclopentanone was equilibrated to room temperature over night by storing it in the fume hood. SU-8 2100 was weighed out and mixed with cyclopentanone by manual stirring with a glass rod until a uniform viscosity was achieved. SU-8 2003.5 was stored in a light-secured bottle at room temperature in the cleanroom. SU-8 5 (Microchemicals) was provided in the cleanroom.

4” silicone wafers were cleaned by soaking in acetone before rinsing with isopropanol, ethanol and DI water. The wafer was then dried with  $\text{N}_2$  (g) to remove any solvent. The rinsed substrate was inspected under the microscope to ensure that there were no contaminants. The wafer was plasma cleaned to improve resist adhesion. Plasma cleaning was performed for 2 minutes with 50 %  $\text{O}_2$  and 50 % generator power. This was followed by a 10-minute dehydration bake at 180  $^\circ\text{C}$  to remove any remaining solvents.

Photoresist was applied to the wafer by spin coating. SU-8 2003.5 was spun to a thickness of 2.3  $\mu\text{m}$  and SU-8 5 was spun to a thickness of 3.8  $\mu\text{m}$ . Spin parameters for the resists are given in table 1-1.

**Table 4-1. Photoresists and optimized spin parameters for photolithography.**

Photoresist	Spread cycle			Spin cycle			Film thickness ( $\mu\text{m}$ )
	Speed (rpm)	Acceleration (rpm/s)	Time (s)	Speed (rpm)	Acceleration (rpm/s)	Time (s)	
SU-8 2003.5	500	200	5	3000	1000	35	1.4
SU-8 5	500	200	5	5500	1000	35	4.8

After spinning, the coated wafer was first baked at 65  $^{\circ}\text{C}$  for 1 minute, the hot plate was ramped up to 95  $^{\circ}\text{C}$  and kept at the maximum temperature for 1 minute for the SU-8 2003.5 and for 3 minutes for SU-8 5. The photoresist thickness was measured using a Filmetric thin film measure (Filmetric).

The substrate was exposed to UV light at 365 nm in a UV mask aligner (MA/BA6 mask aligner, Karl Süss, Germany) with hard contact and a 30  $\mu\text{m}$  alignment gap. SU-8 2003.5 was exposed at an exposure dose of 60  $\text{mJ}/\text{cm}^2$  and SU-8 5 was exposed at 140  $\text{mJ}/\text{cm}^2$ . Exposure time was calculated from the formula

$$\text{Exposure time} = \frac{\text{Exposure dose}}{\text{Lamp intensity}}$$

After completed exposure, the substrate is subjected to a post-exposure bake. The substrate is first baked at 65  $^{\circ}\text{C}$  for 1 minute, before the hot plate was ramped up to 95  $^{\circ}\text{C}$  and kept at the maximum temperature for 1 minute for both resists. The substrate was then slowly cooled to room temperature on a cooling hot plate to prevent thermal stress in the resist film.

The substrate was developed in mrDev-600 (Microchemicals) for 1 minute under constant agitation before rinsing in fresh developer, isopropanol and drying with  $\text{N}_2$ . An overview of the photolithography process is given in figure 4.2-1.

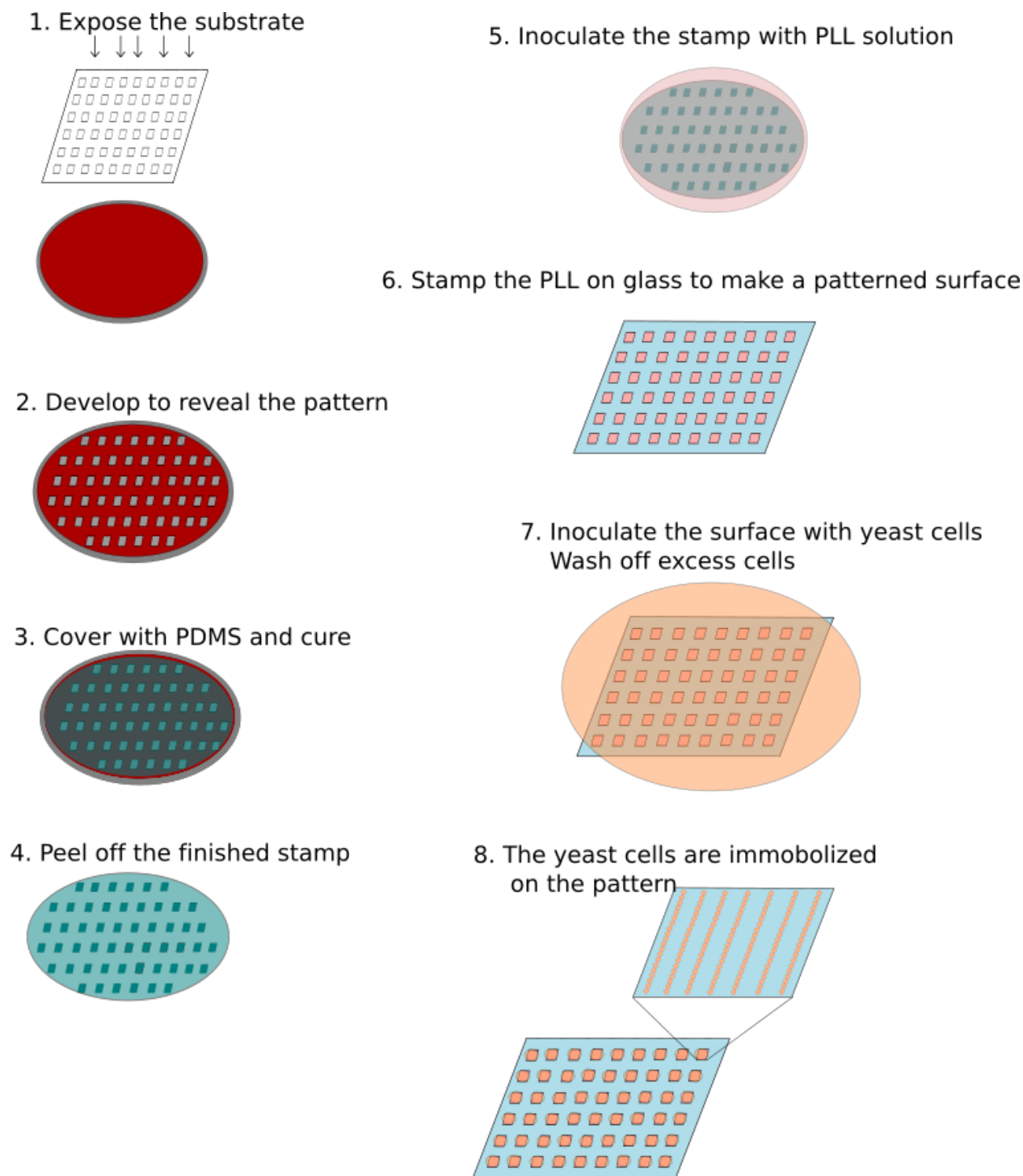


**Figure 4.2-1. Overview of the microcontact printing procedure for cell immobilization.**

### **4.3. Replica moulding**

PDMS pre-polymer Sylgard-184 (Dow Corning) and curing agent (Dow Corning) were mixed at a 1:10 ratio by weight. Approximately 27 g of pre-polymer and 2.7 g of curing agent were used for a 4" wafer in an aluminium holder. The pre-polymer and the curing agent were

mixed briefly using a plastic spoon before de-gassing in a vacuum chamber for 5-7 minutes to remove any bubbles. The mixture was carefully poured onto the wafer by hand. PDMS was cured in a curing oven at 85 °C for 2 hours. The complete mould was carefully peeled off the stamp using tweezers.

#### **4.4. Stamp characterization**

##### **μCP of fluorescent molecules**

Hydrophilic qualities of the PDMS stamps were increased through plasma cleaning for 1 minute with 50 % O<sub>2</sub> and 50 % generator power. This step had to be performed immediately before the stamping because the effect is temporary. For characterization of the stamp surface, 50 μl PLL-FITC (0.5mg/mL in milliQ, Sigma Aldrich) was applied to each array with a pipette. The ink was incubated on the stamp for 15 minutes before excess solution was pipetted off. The stamp surface was dried completely using N<sub>2</sub> (g). Glass slides were cleaned by soaking in acetone and rinsing with ethanol and milli-Q water before drying with N<sub>2</sub> (g). Willco dishes were assembled according to the instructions given by the manufacturer. The stamp was placed pattern-side down on the clean glass substrate using two pairs of tweezers. Air between the stamp and the glass substrate were carefully removed using the tweezers. Weights of 100 g were applied to the stamp to ensure proper contact between the stamp and the surface.

##### **Atomic force microscopy of stamp surface**

AFM analysis of the stamps was performed by Gjertrud Maurstad (Institute of Physics, NTNU). An atomic force microscope was used to study the stamp surface and characterize the shape and height of the features.

#### **4.5. μCP**

Hydrophilic qualities of the PDMS stamps were increased through plasma cleaning for 1 minute with 50 % O<sub>2</sub> and 50 % generator power. 50 μl PLL (0.01 %, Sigma Aldrich) was applied onto the array area of the PDMS stamp and incubated for 15 minutes. Excess solution was pipetted off and the stamp was dried using N<sub>2</sub> (g). The dried stamp was placed pattern side down on a cleaned glass substrate and 100 g weights were applied for 10 minutes. The

stamp was carefully peeled off. A 100  $\mu$ l solution of yeast cells was applied to the patterned area and incubated for 10 minutes before washing the slide in MilliQ-water to remove unattached cells. The washing was repeated until any visible yeast cells were removed. The immobilized cells were inspected under a Zeiss Axiobserver Z.1 microscope using phase contrast.

Yeast cells were also immobilized on glass slides functionalized PLL with no pattern to verify adhesion. 100  $\mu$ L of PLL (0.01%) was added to a cleaned glass slide and incubated for 10 minutes. Excess solution was pipetted off and the slide was dried with N<sub>2</sub> (g). The re-suspended yeast cell solution was added to the glass slide and incubated for 10 minutes before gently washing with MQ water until any visible cells were removed. The immobilized cells were inspected under a Zeiss Axiobserver Z.1 microscope using phase contrast.

#### **4.6. Yeast cell inoculation and processing**

*Saccharomyces cerevisiae* was cultivated on agar plates with YPD and stored in a cool storage room (4 °C) between experiments. Cells were inoculated in 25 mL YPD medium (35 °C, 180 rpm) for at least 12 h before immobilization experiments. The overnight culture was then up-concentrated and washed to remove YPD because the medium contains yeast cell extracts that will interfere with the interaction between YPD and PLL. 2 ml of overnight culture were extracted into an Eppendorf tube and centrifuged for 5 minutes at 4000 rpm. The supernatant was discarded and the pellet was re-suspended in 100  $\mu$ l of MOPS buffer (10 mM, pH 7) and centrifuged for 5 minutes at 4000 rpm. The cleaning step was repeated two more times. The supernatant was discarded and the pellet was re-suspended in 500  $\mu$ l MOPS buffer.

## 5. Results and discussion

The thesis work was focused on developing a method for  $\mu$ CP of poly-L-lysine on a glass surface with the end goal of immobilizing *S. cerevisiae* on the functionalised surface. The result section will be made up of a description of how each distinct step of the method was developed and improved as well as a description of the final developed method.

The method used for microcontact printing was based on work performed by Nina Bjørk Arnfinnsdottir at NTNU as part of her doctoral thesis where she made bacterial microarrays (52) as well as work by Åshild Samseth as part of her master thesis where she immobilized *S. cerevisiae* on non-patterned glass surfaces coated with PLL (44).

### 5.1. Starting point

It was verified that PLL (0.01 %) coated on glass surfaces could be used to immobilize *S. cerevisiae* and it was demonstrated that the cells adhered poorly to clean glass slides. This meant that passivation of the glass surface was not considered necessary (44). Nina Bjørk Arnfinnsdottir was able to immobilize *Pseudomonas putidas* on 3  $\mu$ m spots of polydopamine. Her work also demonstrated that it was possible to pattern PLL-FITC using a micrometre scale pattern on a PDMS stamp (52). I had access to the photomasks that were used by Nina Bjørk Arnfinnsdottir in her PhD work and attempted to recreate her results with *P. putidas* on PD with *S. cerevisiae* on PLL.

### 5.2. Method overview

The method consists of four separate main steps: photolithography, replica moulding, microcontact printing and immobilization of yeast cells. Several aspects of each of the steps need to be optimized for the specific requirements for this project. The main points where optimization was needed are described below.

In photolithography, several parameters can be modified to get the desired results. Firstly, the cleaning procedure must be optimized. The type of solvents used, whether to include a plasma-cleaning step and the duration and temperature of a dry bake are important to achieve a clean substrate before spinning. Choosing the photoresist with the correct viscosity for the desired features is the next important step. Film thickness depends on photoresist viscosity

and spin parameters. The maximum spin speed, acceleration and spread cycle parameters must be optimized to achieve the correct film thickness and prevent artefacts during spin coating. Thermal curing of the resist must also be optimized. Soft bake and PEB temperature as well as ramp rate and cool-down must be adapted to prevent thermal stress. Exposure type and dose as well as development time and agitation must also be optimized to produce a good master mould.

Some optimization is also required for replica moulding. Whether to silanize the surface and if so what silanization agent to use to preserve the master mould should be considered. When using the PDMS, the polymer: curing agent ratio, mixing time, degassing time, amount of PDMS mixture used per wafer, curing time and curing temperature can be adjusted to produce stamps with the desired characteristics.

Developing a method for  $\mu$ CP also requires that some parameters be optimized for the specific procedure. The elastomer stamp can be modified in several ways to make the surface more hydrophilic, and both temporary modifications through plasma cleaning and permanent changes through bonding functional groups to the stamp surface are possible. Other parameters that can be optimized are the amount of the “ink” solution that should be applied and whether it should be applied to the entire surface or only the array areas, how much of the stamp that should be utilized for each time, how much pressure should be applied to the stamp during  $\mu$ CP such as manual pressure or using a weight, duration of stamping, and whether the stamp can be cleaned and re-used. Strategies for verifying that the correct pattern has been transferred should be developed. Options include stamping a fluorescently tagged molecule or using AFM to directly visualize the stamp surface.

Immobilization of *S. cerevisiae* requires that the growth medium needs to be removed from the cells to immobilize on PLL, as the interaction is based on charge and is not specific. The method established by Åshild Samseth was a centrifugation based cleaning of the cells, before adding a buffer that is suitable for viable cells (44). A suitable amount of cell solution to add and how long the solution should be left on the surface must be determined. It should also be established e how non-immobilized cells should be removed from the array without destroying the array surface.

### 5.3. Photolithography optimization

Using the two negative tone photoresist SU-8 2003.5 and SU-8 5 (Microchemicals), optimization of all the previously described photolithography parameters was attempted to create a master mould for replica moulding.

#### 5.3.1. Process optimization for SU-8 2003.5

Based on achieved photoresist thickness by Nina Björk Arnfinnsdottir, SU-8 2003.5 was chosen as the photoresist most suitable for the used pattern. A thickness of approximately 2.3  $\mu\text{m}$  was achieved consistently using the resist SU-8 2 (52), which was not available in the cleanroom at this point in time. The resist SU-8 2003.5 has a 37 % solid content and was used to replace the SU-8 2 because it has similar characteristics. The basic cleaning procedure that was applied to the silicone wafer was soaking in acetone and flushing with IPA, ethanol and DI water. It was thoroughly dried using a stream of clean  $\text{N}_2$  (g) and the wafer was dry-baked on a hotplate at 180 degrees for 15 minutes to remove any remnants of the solvents. The achieved film thickness for SU-8 2003.5 at different spin speeds is given in table 5-1.

**Table 5-1. Spin parameters and achieved film thickness for SU-8 2003-5 photoresist.**

Spread cycle			Spin cycle			Thickness ( $\mu\text{m}$ )
Spin speed (rpm)	Acceleration (rpm/s <sup>2</sup> )	Duration (s)	Spin speed (rpm)	Acceleration (rpm/s <sup>2</sup> )	Duration (s)	
500	200	5	1800	1000	30	1.4

Several artefacts were observed on the substrate using the described method. Comets and pinholes were observed in the resist film during soft bake. The artefacts could be a result either of particle contamination on the substrate surface after cleaning or the presence of bubbles in the resist as a result of the application process. Application could not be modified significantly given the reaction conditions available, thus the cleaning process became the target for any subsequent method modifications.

The substrate was exposed to UV-light in a mask aligner (MA/BA6 MaskAligner, Karl Süss, Germany) using hard contact exposure due to the size and shape of the features. The initial exposure dose was based on the recommended exposure dose for a 2  $\mu\text{m}$  thick resist film of SU-8 2 (30), as the resists have a similar solid content. At an exposure dose of 60  $\text{mJ}/\text{cm}^2$ , the resist appeared well exposed. The surface was not cracked and the features were clearly

defined and visible after post-exposure bake. The exposure dose was not further adjusted. During development of the wafer, a white coating appeared on the resist surface during flushing with isopropanol. After re-submerging the wafer in developer for additional time and flushing with fresh developer, the residue was still clearly visible on the surface.



**Figure 5.3-1. Silicone wafers with SU-8 2003.5 covered in residue formed after development in MrDEV-600.** The patterns shown are (a)  $10 \times 10 \mu\text{m}$  squares with a  $10 \mu\text{m}$  separation distance and (b)  $8 \mu\text{m}$  stripes with an  $8 \mu\text{m}$  separation distance. The images were obtained using a Nikon Eclipse LV150 microscope.

### 5.3.2. Process optimization for SU-8 5

As the pattern used contained features in the micrometre scale, the risk of roof collapse was considered small and higher features were attempted. Also wanted to use a pre-mixed resist from the cleanroom to increase reproducibility of the result as it was difficult to properly mix cyclopentanone with the thicker resist. The self-mixed resist appeared to have an uneven viscosity, as there was variation in the thickness when using the same resist at different spin speeds. The resist was substituted with SU-8 5 to get a feature height closer to 5  $\mu\text{m}$ , which was the suggested film thickness at 3000 rpm (30). Different spin speeds were attempted to achieve the desired spin speed with an even resist coating (table 5-2).

**Table 5-2. Spin speed and film thickness for SU-8 5 photoresist on 4” silicon wafers.**

Spread cycle			Spin cycle			Thickness ( $\mu\text{m}$ )
Spin speed (rpm)	Acceleration (rpm/s <sup>2</sup> )	Duration (s)	Spin speed (rpm)	Acceleration (rpm/s <sup>2</sup> )	Duration (s)	
500	200	10	6000	1000	35	3.8
500	200	10	3000	1000	35	4.8
500	200	10	5500	1000	35	3.2

A starfish pattern of resist on the wafer was observed initially, indicating a too low amount of resist applied. Increasing the amount of resist used from 3 ml to 4 ml enabled an even coating of resist across the entire 4” silicone wafer. An initial spin speed of 6000 rpm gave an even coating of resist, but a film thickness that was significantly thinner than what was desired. Modifying the cleaning procedure increased the film thickness to 3.8  $\mu\text{m}$ . The time of soaking the silicone wafer in acetone was increased to 2 minutes under agitation and flushing with solvents was performed more carefully and the wafer was inspected under the microscope after cleaning to ensure that it was entirely clean. This improved the appearance of the wafer improved and there was a decreased amount of comets and pinholes on the surface. A plasma-cleaning step was also added to the cleaning procedure in order to improve resist adhesion to the surface and improve uniformity across the silicone wafer.

The spin speed was decreased to 3000 rpm according to the recommended spin speed in the accompanying data sheet (30). Reduced spin speed resulted in a film thickness increased to 4.8  $\mu\text{m}$ , which was close enough to the desired value to be considered acceptable. Artefacts that had not been observed with the initial spin parameters appeared. An edge bead was

observed when decreasing the spin speed to increase resist thickness. The lowered spin speed also gave the appearance of a “tidemark” of dried resist around the area where the resist had been applied prior to spinning (figure 5.3-2). The boundary of the tidemark was measured to be thicker than the surrounding resist. It was attempted to avoid the formation of a tidemark by starting the program on the spinner before applying the resist so that the program begins running immediately once the lid is shut and the vacuum is applied. However, this modification did not reduce appearance of the tidemark (Figure 5.3-2).

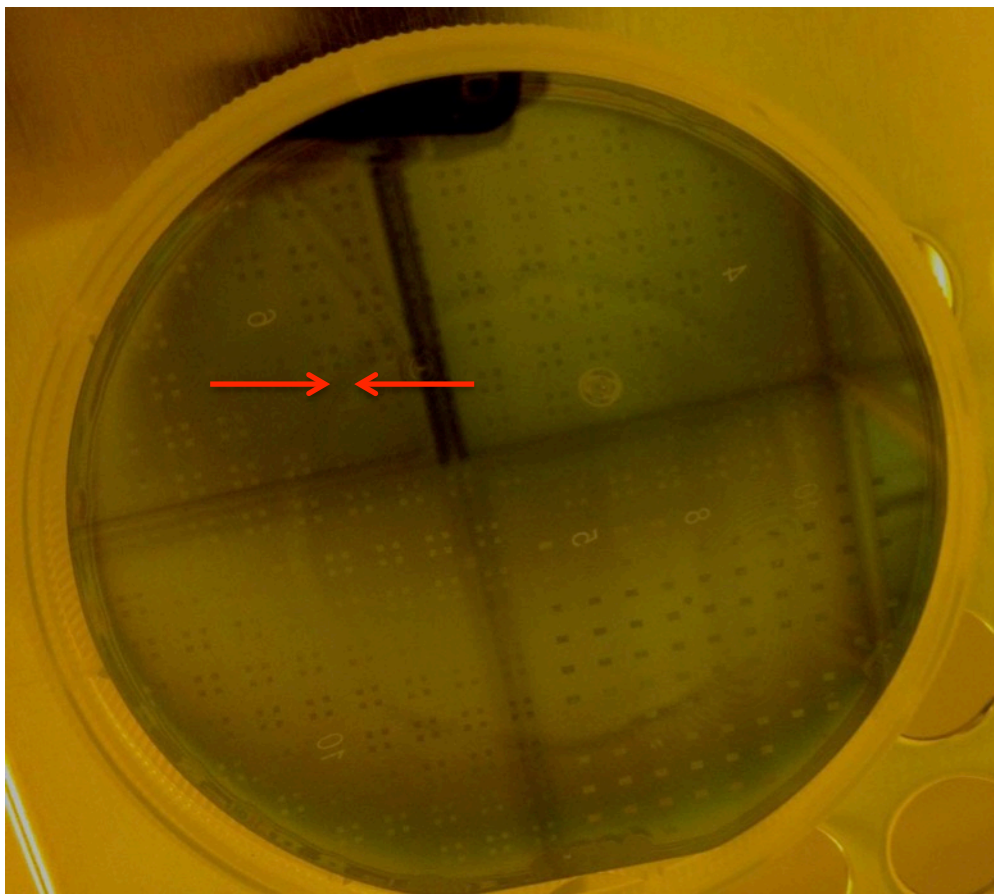


**Figure 5.3-2. Tidemark of dried photoresist on 4” wafer with SU-8 5 photoresist.** The tidemark appeared around the area where the resist was initially applied to the wafer before spinning.

By increasing the maximum spin speed from 3000 rpm to 5500 rpm, the film thickness decreased from 4.8  $\mu\text{m}$  to 3.8  $\mu\text{m}$  and the tidemark disappeared. The occurrence of the edge bead was also decreased.

Some irregularities appeared during the soft bake, but they were not considered to be caused by the soft bake conditions. During heating, solvent evaporates out of the photoresist and as it solidifies the unevenness that is already present becomes visible to the naked eye. The method

used soft bake as recommended for the resist, as the result of this seemed satisfactory and the post exposure bake is considered most important for introducing stress (32).

### Exposure dose

Exposure of the 4.8  $\mu\text{m}$  thick resist film was performed using hard contact and a 120  $\text{mJ}/\text{cm}^2$  gave an uneven exposure where certain areas were strongly overexposed to the degree where there were large holes in the resist film while other areas of the substrate were well defined with regular features (figure 5-3).

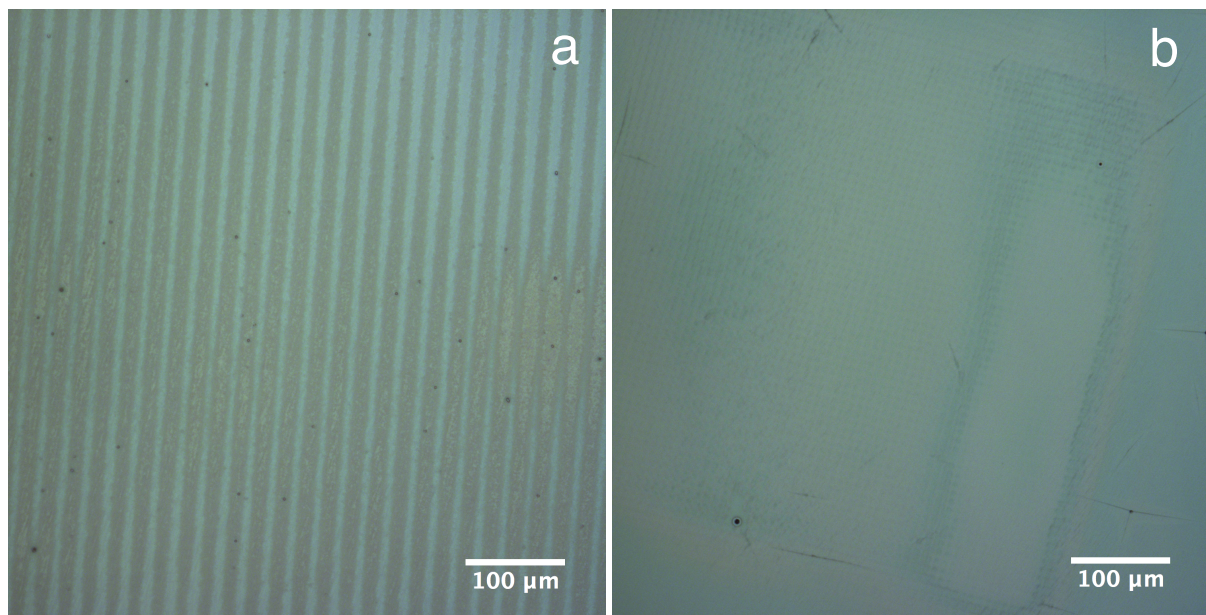


**Figure 5.3-3. SU-8 5 photoresist (3.8  $\mu\text{m}$  film thickness) exposed at 120  $\text{mJ}/\text{cm}^2$ .** There was an uneven exposure, as can be seen from the uneven thickness of the stripes (a) and the hole in the resist layer (b). Images were obtained using a Nikon Eclipse LV150 microscope.

An exposure series was performed to determine the appropriate exposure dose. Based on a recommended dose of 140  $\text{mJ}/\text{cm}^2$ , doses of 100, 120 and 140  $\text{mJ}/\text{cm}^2$  for a resist thickness of 3.8  $\mu\text{m}$ . 140  $\text{mJ}/\text{cm}^2$  recommended for a 5 $\mu\text{m}$  coating of SU-8 5, went below due to having a thinner layer.

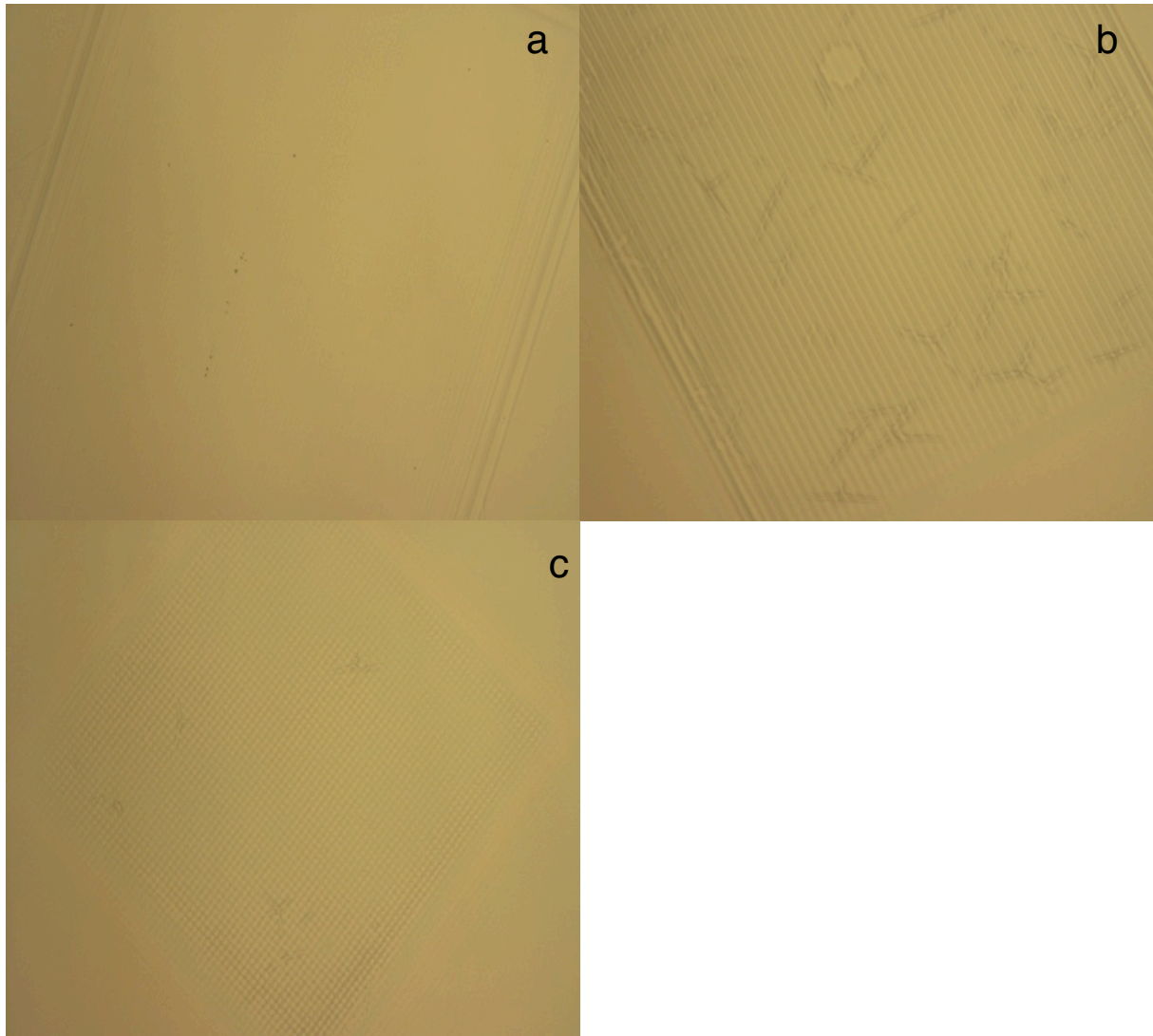


**Figure 5.3-4. SU-8 5 photoresist (3.8 μm film thickness) exposed at different exposure doses.** (a) exposed at 100 mJ/cm<sup>2</sup> with a 8 μm stripe pattern with 8 μm separation distance, (b) exposed at 120 mJ/cm<sup>2</sup> with a 8 μm stripe pattern with 8 μm separation distance and (c) exposed at 140 mJ/cm<sup>2</sup> with a 6x6 μm square pattern with 6 μm separation distance. Images were obtained using a Nikon Eclipse LV150 yellow light microscope.

Exposure at 120 mJ/cm<sup>2</sup> gave the best-defined pattern for the stripes, but the square patterns appear more defined at 100 mJ/cm<sup>2</sup>. Both substrates were used as master moulds for replica moulding.

### **Development**

During development, agitation was applied to the substrate. The type of movement used was initially circular, similar to stirring in a pot. This approach was not effective in removing dissolved resist from the wafer, as some of the dissolved resist landed back on the wafer and caused an uneven coating across the substrate. A wave-pattern could be observed across large

areas of the substrate surface. The areas with visible uneven resist could be measured as thicker than the surrounding areas of resist. Development was modified to a more lateral motion and faster agitation, resulting in a more complete removal of the dissolved resist. However, some wave pattern was still visible on the developed substrate (figure 5-5).

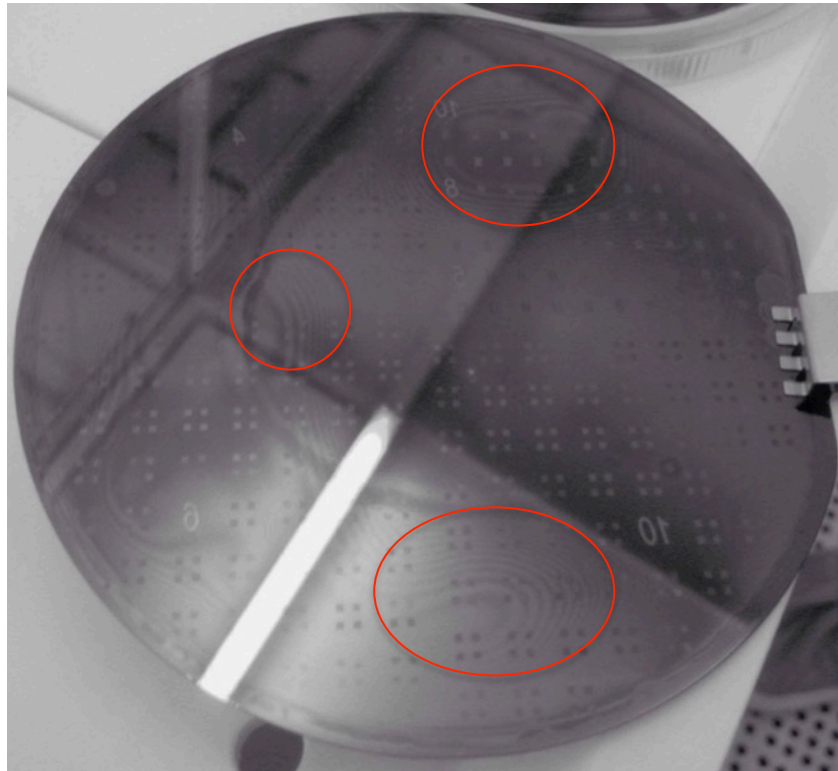


**Figure 5.3-5. Resist residues on the developed wafer after circular agitation.**

### **Remaining challenges**

An edge bead removal step should be added to the procedure to ensure an even resist film. This would improve the quality of the exposure. A spin-off step could be added to the end of the spin coating to see if this would reduce the occurrence of the edge bead. Alternatively, solvent could be added to the outer edge of the wafer to dissolve the edge bead entirely. It would cause some loss of pattern area along the outer edge of the resist, but due to the presence of a significant edge bead this area cannot be used with the current procedure regardless.

The mask design could be modified to be specifically suitable for working with yeast cells. Features on the mask were larger than yeast cells and were not suitable for single cell immobilization, but were chosen mainly because the large features would be easier to

visualize in a developmental stage of the process. Changing the design could also make the stamps easier to work with. The mask used for the pattern circles with varying sizes had the opposite polarity and a design where the entire surface is raised, but the stamp contains lowered pockets where the features are held. This improved the structural integrity of the stamp and made it easier to achieve contact between array and substrate without risking roof collapse.

A different contact mode could be chosen for the exposure. Hard contact exposure was suitable because the feature size of the pattern was fairly large. No features are smaller than 1  $\mu\text{m}$ . However, hard contact brings the wafer into direct contact with the mask repeatedly, increasing the risk of mask contamination. The presence of the edge bead would have an extra large effect when using this type of contact (figure 5.3-6). It could be possible to use soft contact or vacuum exposure for a better result.



**Figure 5.3-6. The effect of edge bead on hard contact exposure.** The edge bead will be brought into contact with the mask, leaving an air gap between the mask and the substrate. There is also significant risk of mask contamination.

Thermal stress was the other major problem experienced with the procedure. Inspecting the substrate between every step revealed that the observed cracks were formed during the PEB and were increased during development. In some cases it was also observed that part of the resist layer loosened completely from the wafer during development. It appeared that the developer came in through the cracks and damaged the integrity of the resist. Thermal stress can be increased by both over- and under-exposure of the resist, but over-exposure seems most likely given the information from the photoresist supplier (30). As the thickness of the resist layer consistently was lower than the desired thickness this would demand a lower exposure dose as well. A possible solution could be to decrease the PEB temperature and instead increase the duration, as PEB temperature is the most important factor for thermal stress in SU-8 films (32). Decreasing the PEB temperature to 55°C was found to decrease residual stress by 70 % (33). The cool-down rate is also found to be very important, as a rapid cool-down could be another source of thermal stress. The cool-down rate should ideally be controlled.

Manual agitation during development was found to be a weakness as it is not completely reproducible and caused uneven results (figure 5.3-5). Ideally, an automated agitation could be used to make this step more consistent. Another possibility would be to wash the substrate in developer rather than submerging it, but this would require a larger amount of developer per wafer.

The spin parameters were complex to optimize as they vary not only between different resist viscosities, but the type of spinner used and the substrate surface. A difference in film thickness was achieved when using different bottles of the same resist with constant spin parameters. SU-8 5 that was initially used had stood on the bench in the cleanroom for some time; possible that this resist was more viscous as solvents would have evaporated slightly over time. Starting a new bottle of resist also required a new round of optimization of spin parameters, which is a clear weakness of photolithography method in general. These variations make the method more complicated to reproduce than ideal. This is a significant problem, as the repeated attempts to optimize the spin coating is time-consuming and uses relatively large amounts of expensive photoresist for each experiment. For industrial scale production, it is not a viable alternative.

There were also some challenges connected to the specific resists chosen. SU-8 2003.5 was mixed manually from a higher viscosity resist (SU-8 2100, Microchemicals) and a thinner. Due to the high viscosity of the original resist, it was difficult to achieve an even viscosity of the mixture. Purchasing a pre-mixed resist solution of the desired viscosity could circumvent this problem. SU-8 5 also showed some weaknesses during thermal curing, which impacted the end results of the replica moulding. Thermal stress during too rapid cool-down can cause cracks to form in the resist surface. During replica moulding, uncured PDMS would fill these cracks to give additional raised features.

#### 5.4. Replica moulding

PDMS and curing agent were mixed at a 1:10 ratio by weight, as it was not considered necessary to make a stiffer mixture based on the height and shape of features used. Elastomer stamps were initially made on moulds with SU-8 2003.5, but the residue that appeared on the master surface was also transferred onto the PDMS stamp and prevented their use for microcontact printing (figure 5.4-1).

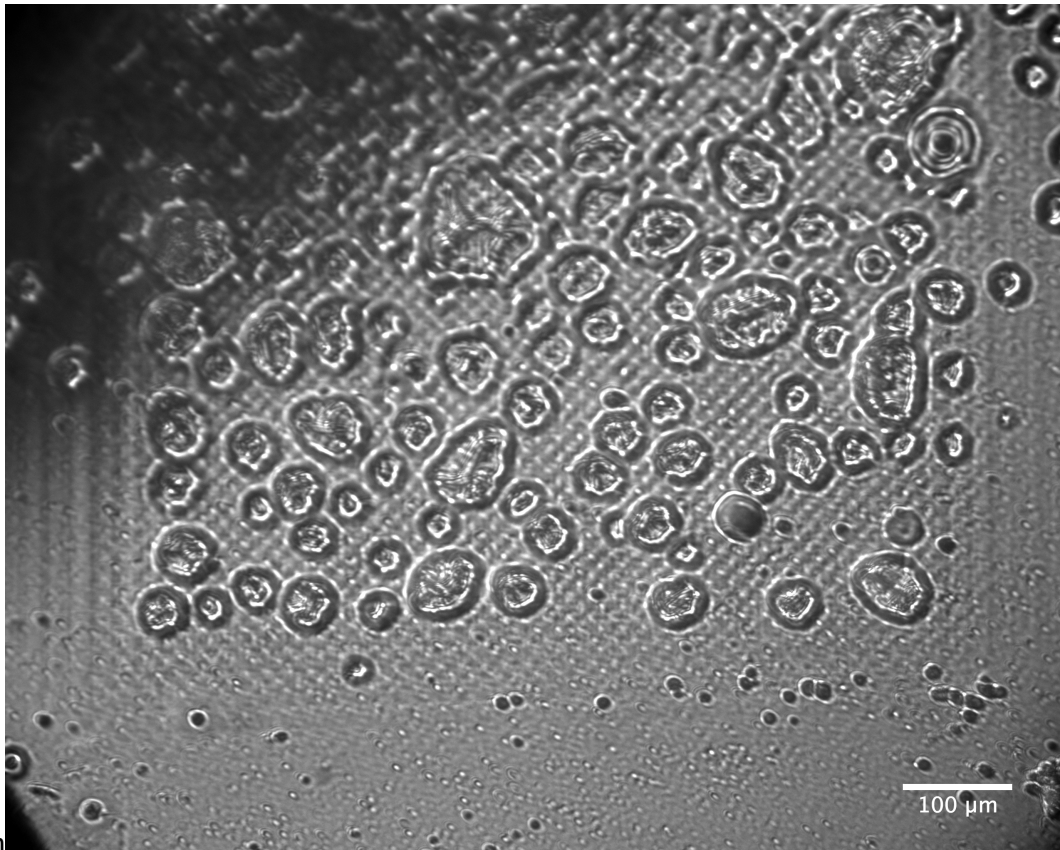


**Figure 5.4-1. PDMS stamp with SU-8 2003.5 photoresist residue on the stamp surface.** The stamp features are 6x6 μm squares with a 6μm separation distance. The image is obtained using phase contrast microscopy on a Zeiss Axiobserver Z.1 microscope.

PDMS was initially cured at 65°C, which required a curing time of 4 hours. The curing temperature was therefore increased to 85°C to reduce the curing time to 2 hours and make the process more efficient. No changes in PDMS characteristics were observed after this change.

### Stamps made from own master moulds

Stamps that were made from non-optimal wafers had flaws that could be recognized from the resist pattern. Cracks in the photoresist surface could also be recognized in the stamp (figure 5-4.2).

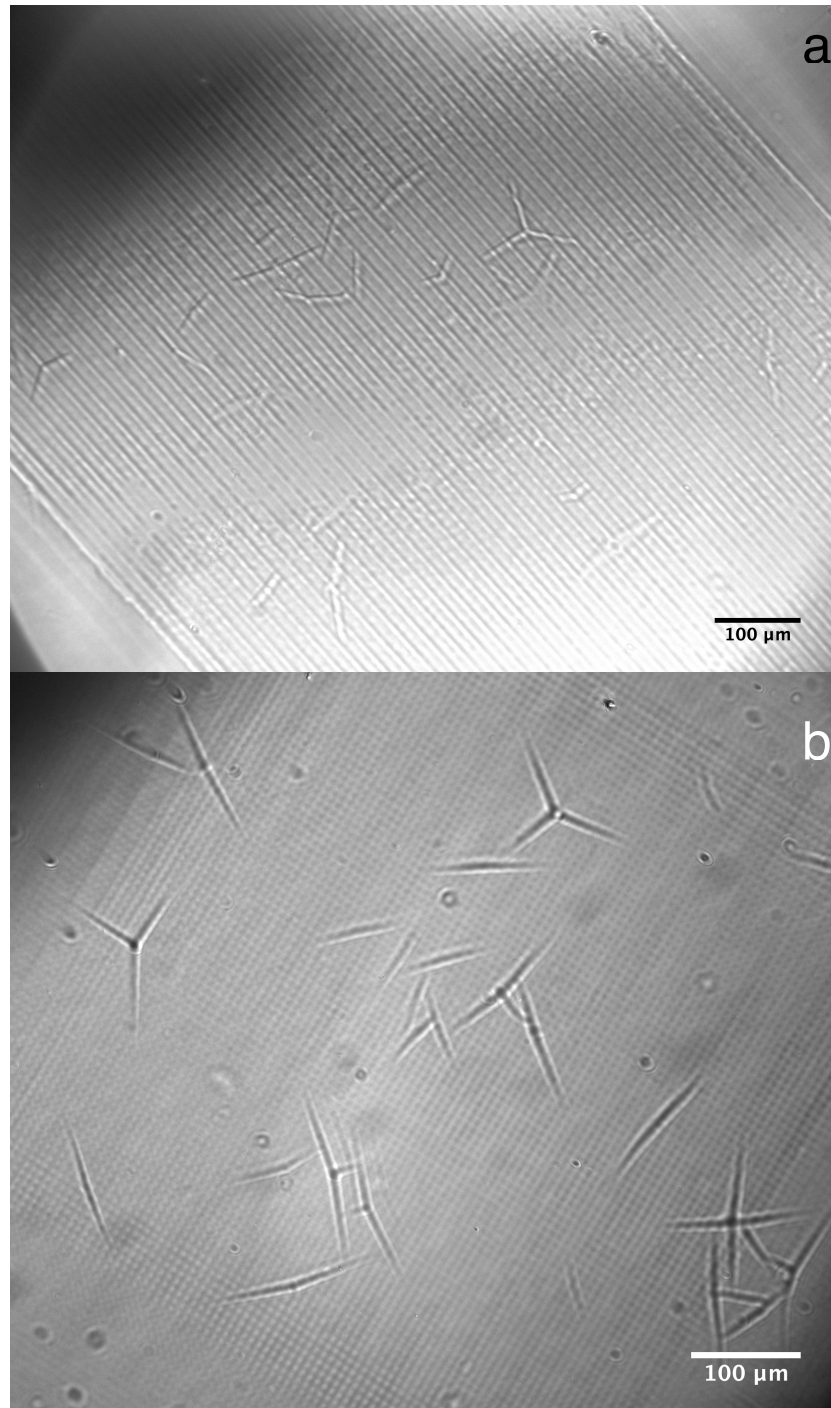


**Figure 5.4-2. PDMS stamps with irregularities on the surface.** The master mould was produced with 4.8 $\mu\text{m}$  layer of SU-8 5 on a 4" silicone wafer, exposed with hard contact lithography at 120 mJ/cm<sup>2</sup>. The pattern is (a) 8  $\mu\text{m}$  stripes with an 8 $\mu\text{m}$  separation distance and (b): 6x6  $\mu\text{m}$  squares with a 6  $\mu\text{m}$  separation distance. The image was obtained using phase contrast microscopy on a Zeiss Axiobserver Z.1 microscope.

Optimizing the photolithography procedure enabled the production of stamps with distinctive features and more uniform surface as could be observed under phase contrast microscopy (figure 5.4-3).

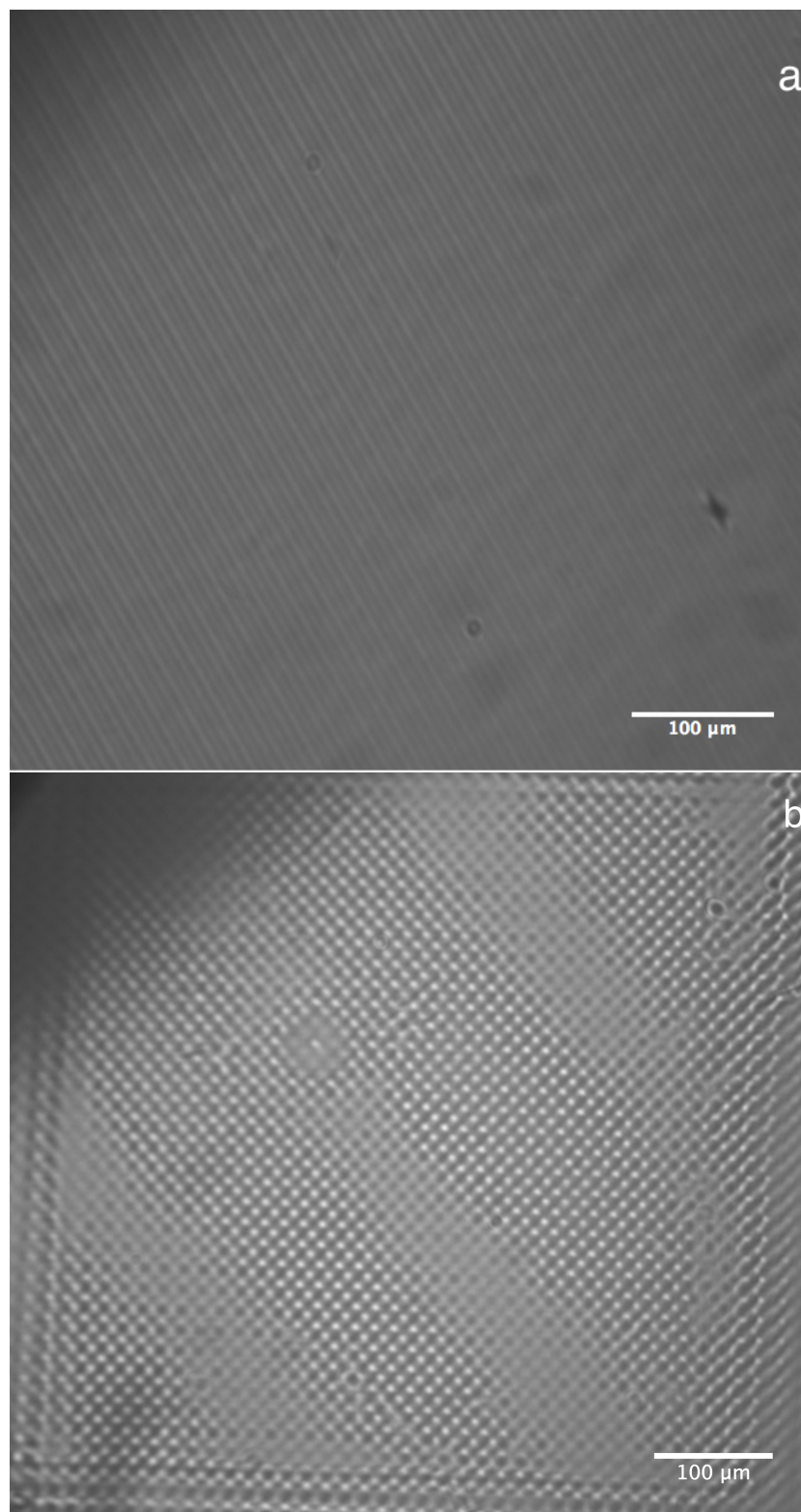


**Figure 5.4-3. PDMS stamps produced with optimized photolithography procedure.** The pattern is (a) 8  $\mu\text{m}$  stripes with an 8  $\mu\text{m}$  separation distance and (b): 6x6  $\mu\text{m}$  squares with a 6  $\mu\text{m}$  separation distance.

PDMS stamps were also made on a master mould provided by Nina Björk Arnfinnsdottir (figure 5.4-4). The pattern on the master was circles with decreasing size (4.4-0.8  $\mu\text{m}$ ) and was not considered suitable for immobilization. It had been verified that the master mould was suitable for stamp production and subsequent  $\mu\text{CP}$  (4, 52) and it was therefore used as a control to verify that the replica moulding process worked.

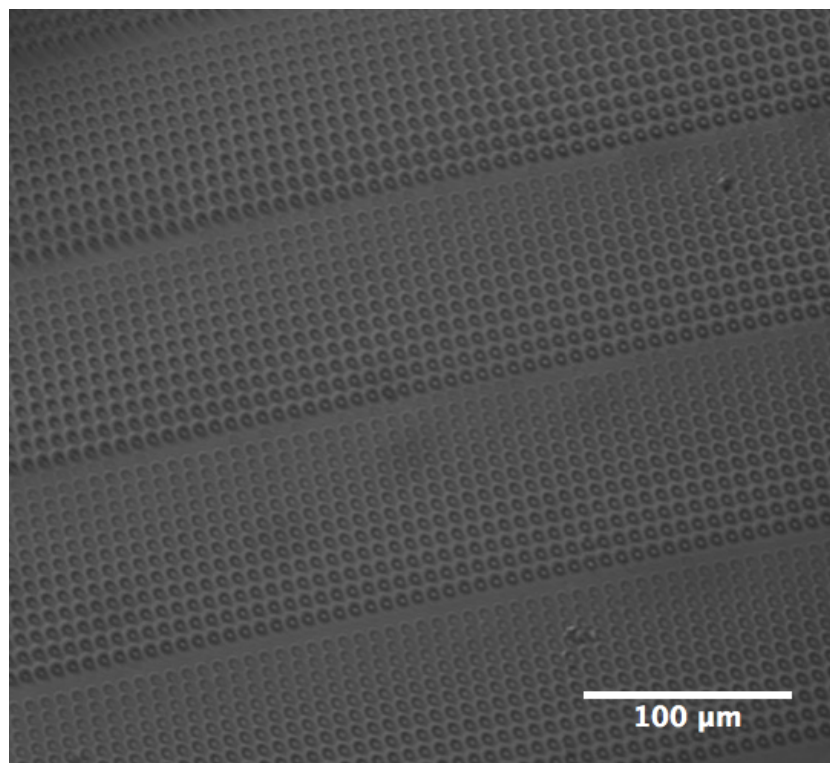


**Figure 5.4-4. PDMS stamp with a pattern of circles with decreasing size (4.4 – 0.8  $\mu\text{m}$ ).** The stamp was made using a pre-made master mould provided by Nina Björk Arnfinnsdottir. Image was obtained using phase contrast on a Zeiss Axiobserver Z.1 microscope.

### **Remaining challenges**

Some master moulds were broken during removal of the stamps due to strong adhesion. Transfer of photoresist to the PDMS was also a problem on occasion, and thus it could be necessary to add a silanization step for a master that would be used several times to prolong the life-time. Irregularities were observed in the stamps. However, there were no indications that the replica moulding process in itself was the source of these problems. Problems from the photolithography procedure were rather recreated in the PDMS. Comparison of the cracks visible on the wafers with irregularities seen on stamps under phase contrast showed that they were in the same pattern. AFM analysis verified that these become raised ridge structures, which would then interfere with  $\mu$ CP.

The presence of bubbles in the PDMS mixture was another challenge. Degassing should ideally not be performed over extended periods of time, as this prolongs the process time significantly. Decreased degassing time led to the presence of bubbles in the finished solution, something that caused irregular structures in the stamp surface. PDMS was applied to the master mould by careful pouring, which could be replaced by application through a syringe to reduce bubbles.

## 5.5. Microcontact printing

The starting point for  $\mu$ CP was trying to visualize the pattern by stamping a fluorescent molecule onto the glass slide. The purpose of this was to show that the pattern observed on the stamp could be accurately transferred to a glass surface. The chemical chosen was PLL-FITC (Sigma Aldrich) since PLL was used for immobilization of yeast cells. Initially, only 3  $\mu$ l of PLL-FITC (0.5 mg/mL in MQ water) was used for each array and the solution was applied specifically to the array areas of the pattern through careful pipetting.  $\mu$ CP with small amounts of ink resulted in poor reproduction of the pattern and low levels of fluorescence. The amount of applied ink was increased to 30  $\mu$ l per array spot, as excess solution is removed after incubation and it was easier to apply larger amounts to the array areas without requiring very careful pipetting to the same degree. This sped up the application process and made it simpler to apply the ink to the desired area of the stamp.

$\mu$ CP when only using mechanical pressure with tweezers and applying 100 g weights on top of the stamp were compared. When only manual pressure was applied, a large amount of smearing on the substrate was observed. It was also difficult to reproduce the type and amount of pressure for repeated experiments, as manual pressure is hard to quantify. Adding the 100 g weight on top of a glass slide on the stamp improved contact between the stamp and the substrate surface and significantly decreased the smearing of the ink (figure 5.5-1).

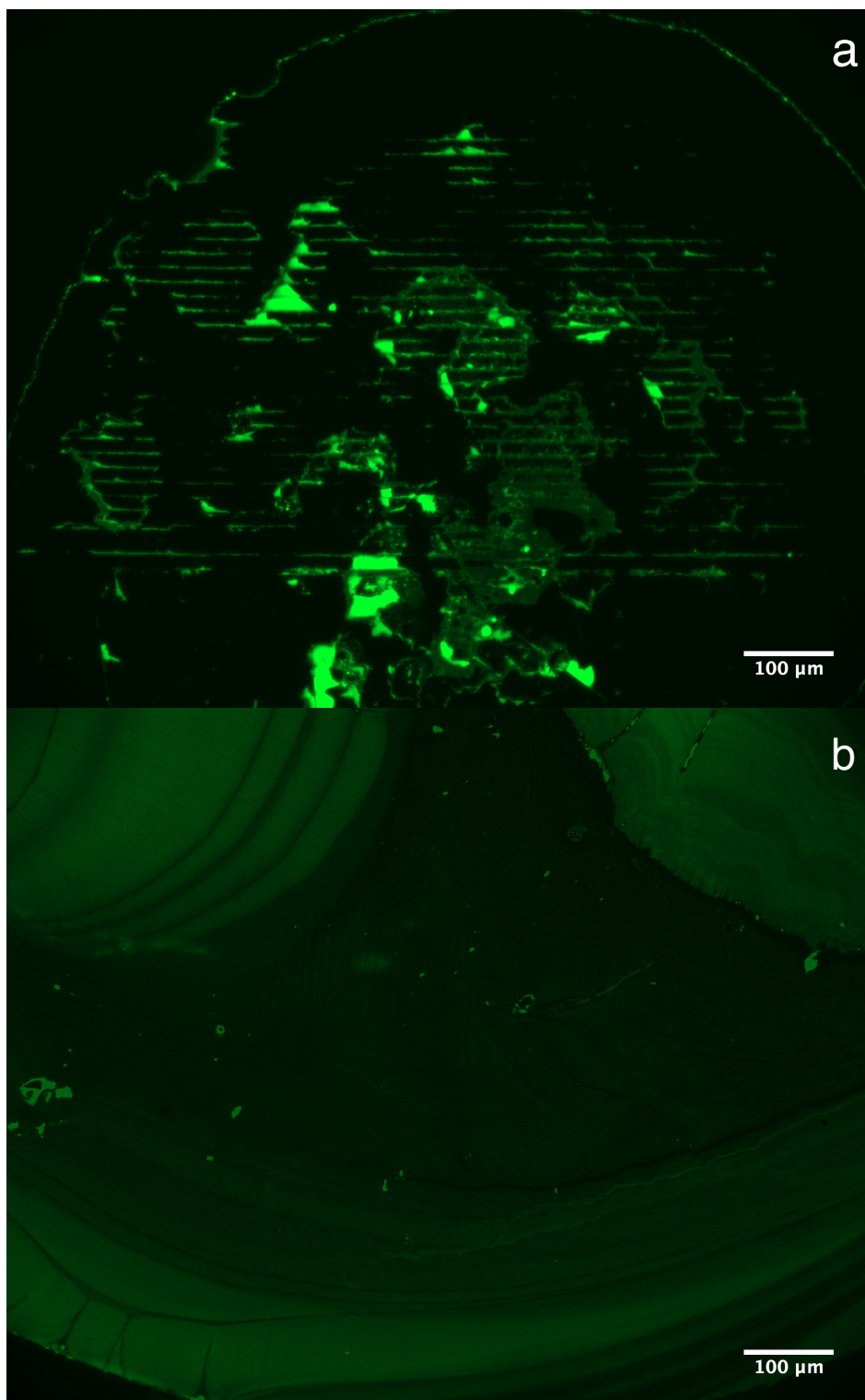


**Figure 5.5-1. Microcontact printing of PLL-FITC on glass substrates (a) with and (b) without applied weight.** A 100 g weight was applied to (a) for 15 minutes during  $\mu$ CP to improve contact with the substrate surface. Stamp (b) was pressed onto the surface using tweezers. The image was obtained using the FITC filter on a Zeiss Axiobserver Z.1 microscope.

The micrometre pattern was partially replicated on the substrate surface. Some areas of the pattern showed visible cracks corresponding to the irregularities observed on the stamp surface structure (figure 5.5-2).

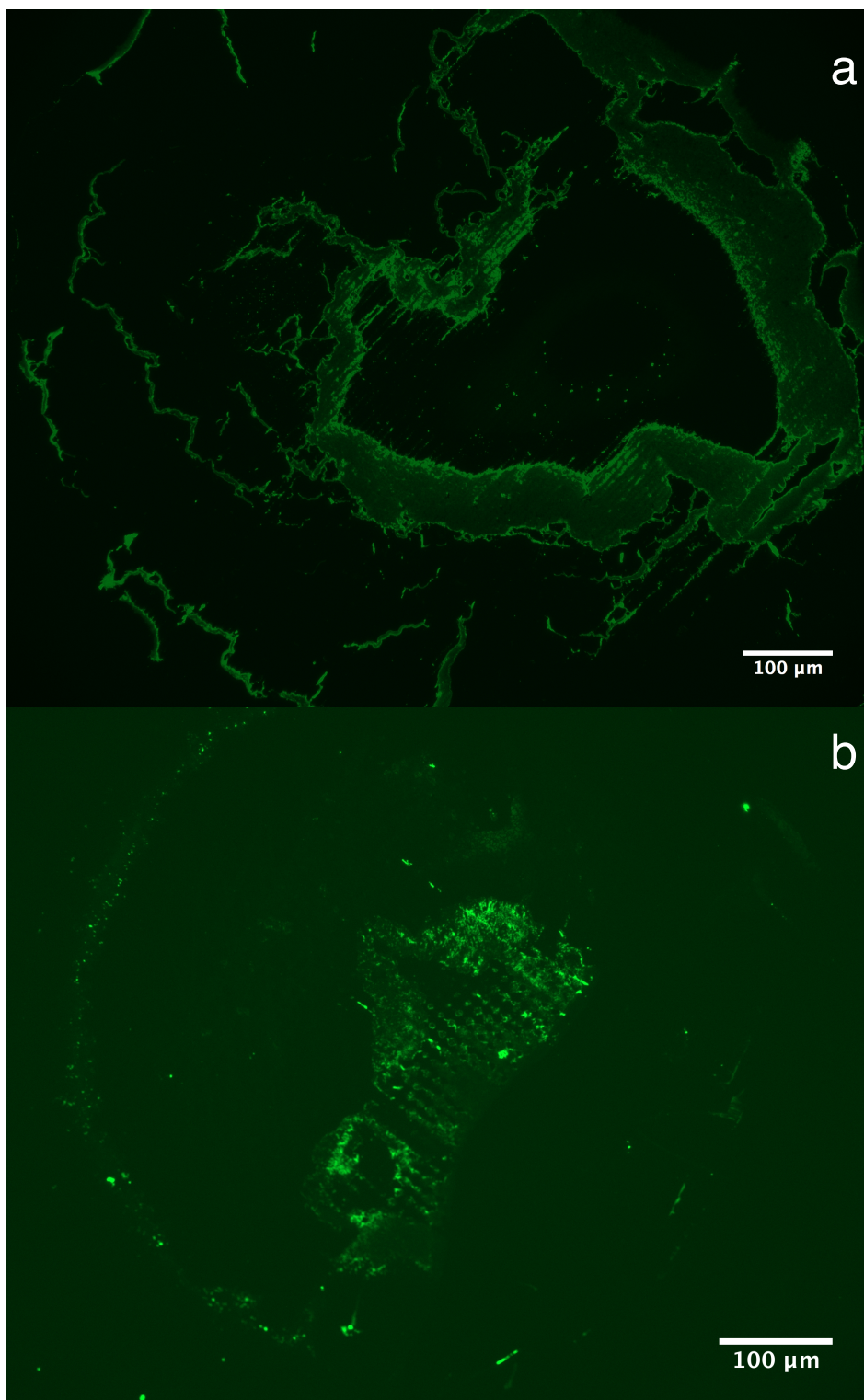


**Figure 5.5-2. Partial stamping of PLL-FITC after  $\mu$ CP.** Pattern on stamp (a) is 8  $\mu$ m wide stripes with 8  $\mu$ m separation distance. Pattern stamp (b) is 6x6  $\mu$ m squares with a 6  $\mu$ m separation distance. The image was obtained using the FITC filter on a Zeiss Axiobserver Z.1 microscope.

The PDMS stamps with the circles in varying sizes design were used as a control to determine whether the  $\mu$ CP procedure could work with a different design.  $\mu$ CP of the circles of varying sizes design showed that the method used enabled the stamping of micrometre scale patterns on untreated glass substrates. A plasma-cleaning step was added to the procedure to temporarily modify the PDMS surface and make it more hydrophilic. This gave a change in surface characteristic and interaction with the PLL-solution, which spread evenly across the entire stamp surface. A smaller amount of solution could be added and would cover the entire stamp. The plasma cleaning also improved the adhesion of PLL-FITC to the stamp and increased the transfer of ink to the glass substrate (figure 5-5.3).

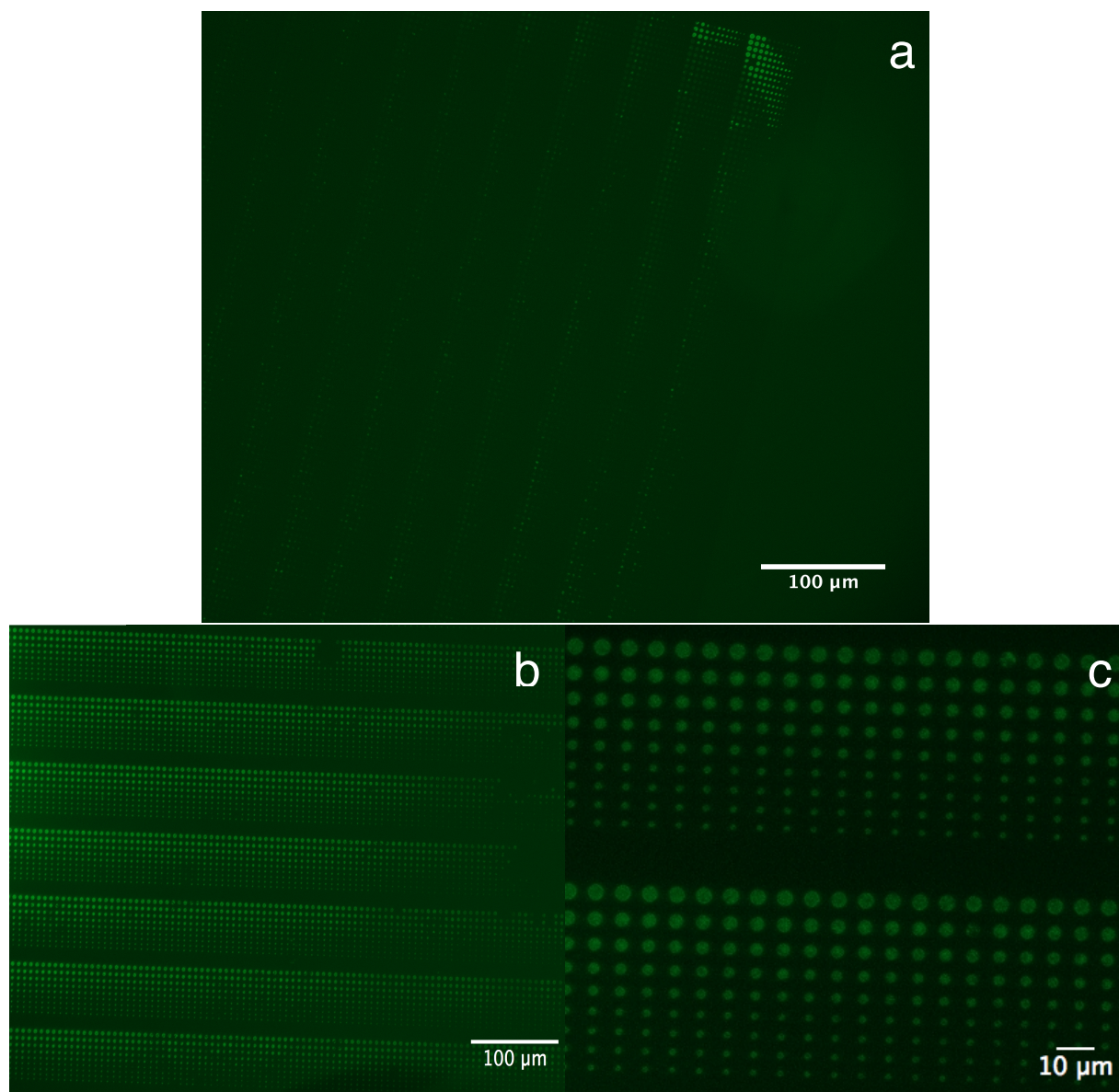


**Figure 5.5-3. Comparison of non-plasma treated (a) and plasma treated (b) PDMS stamp for  $\mu$ CP of PLL-FITC. (c) shows a more detailed image of the pattern created from the plasma treated stamp. The images were obtained using the FITC filter on a Zeiss Axiobserver Z.1 microscope**

## **Remaining challenges**

Reproducibility of the method is challenging because much of it comes down to being careful in the handling of the stamp. When different people perform the same procedure, variations in results could occur. Adding a specific weight to improve contact helps reduce this variability compared to applying pressure to the stamp manually.

The surface of the PDMS is very hydrophobic, making it difficult to apply the PLL solution to the array areas. Very specific pipetting was required, a process that was time consuming and error-prone. The drops of solution pulled away from the PDMS surface and would not properly cover the array. Larger amounts of PLL solution therefore had to be applied to get drops big enough to cover the entire array, which also meant that evaporating off the excess solution took more time. Plasma treatment is a possible way of making the stamp surface more hydrophilic and was shown to be efficient. However, the change is temporary and the effect disappears after approximately 2 hours. Thus, plasma modification must be performed before each  $\mu$ CP experiment. Modification kits that induce permanent changes to the surface are commercially available and provide an alternative solution (53).

## 5.6. AFM analysis of stamp surface

AFM analysis of the PDMS surface was performed to identify factors causing problems with the  $\mu$ CP as well as characterizing the surface structures. Heightened ridges corresponding to the cracks observed on the master moulds were found (figure 5-12).

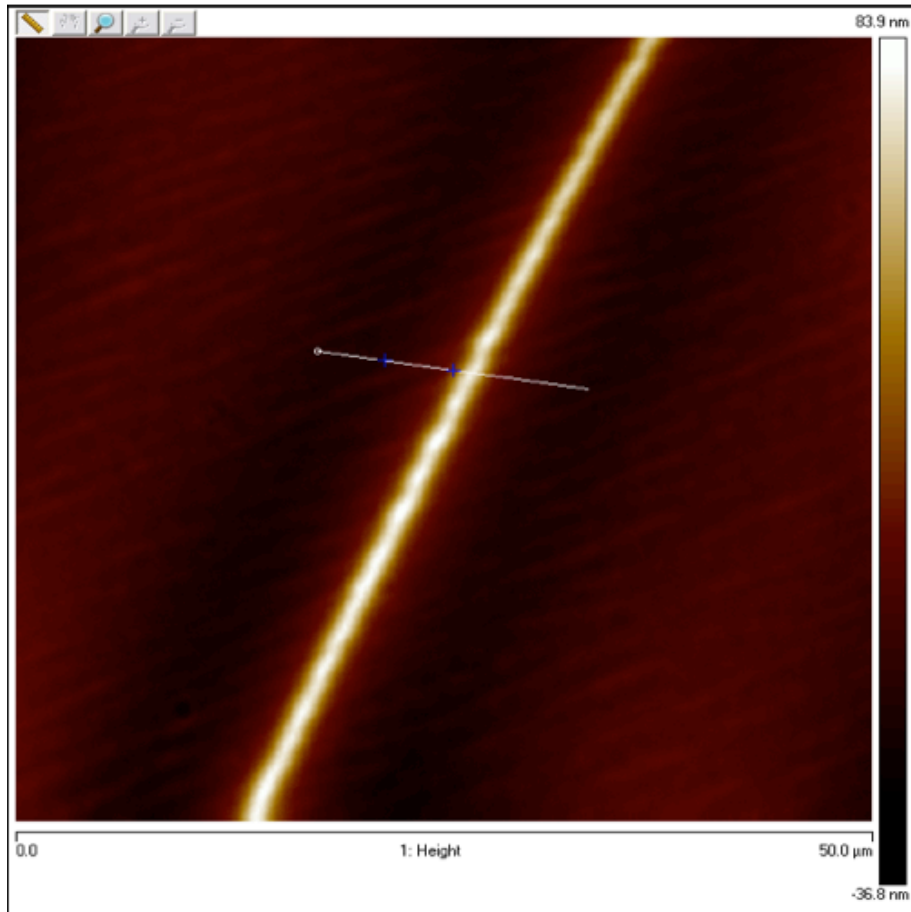


**Figure 5.6-1. AFM height map of PDMS stamp surface.** The master mould is 3.8  $\mu\text{m}$  thick SU-8 5 with a 120  $\text{mJ}/\text{cm}^2$  exposure dose.

Analysis software showed that the ridge in the PDMS was approximately 70 nm in height and 6  $\mu\text{m}$  in width (figure 5.6-2).

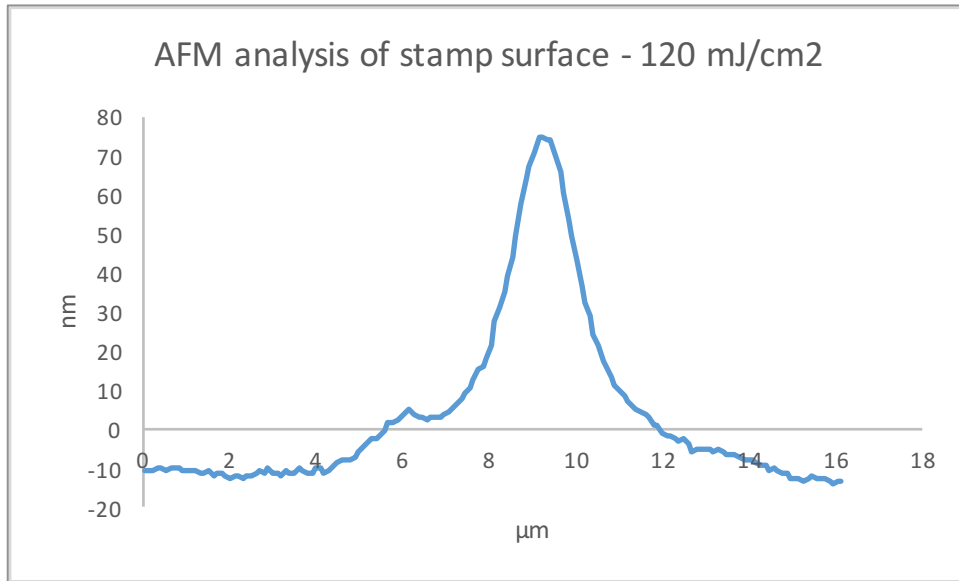


**Figure 5.6-2. Height (nm) and separation (μm) of features on PDMS stamp surface.** The area analyzed corresponds to the line visible on figure 5.6-1.

The ridge was observed to go through a large portion of the PDMS stamp, crossing the array areas. Due to its height compared to the surrounding stamp, the ridge would prevent parts of the stamp close to it from properly touching the surface and would therefore disrupt the pattern during  $\mu$ CP.

Several ridges were observed in the stamp produced from a master mould with a  $140 \text{ mJ/cm}^2$  exposure (figure 5.6-3). AFM analysis showed that the ridges varied slightly in height (figure 5.6-4).

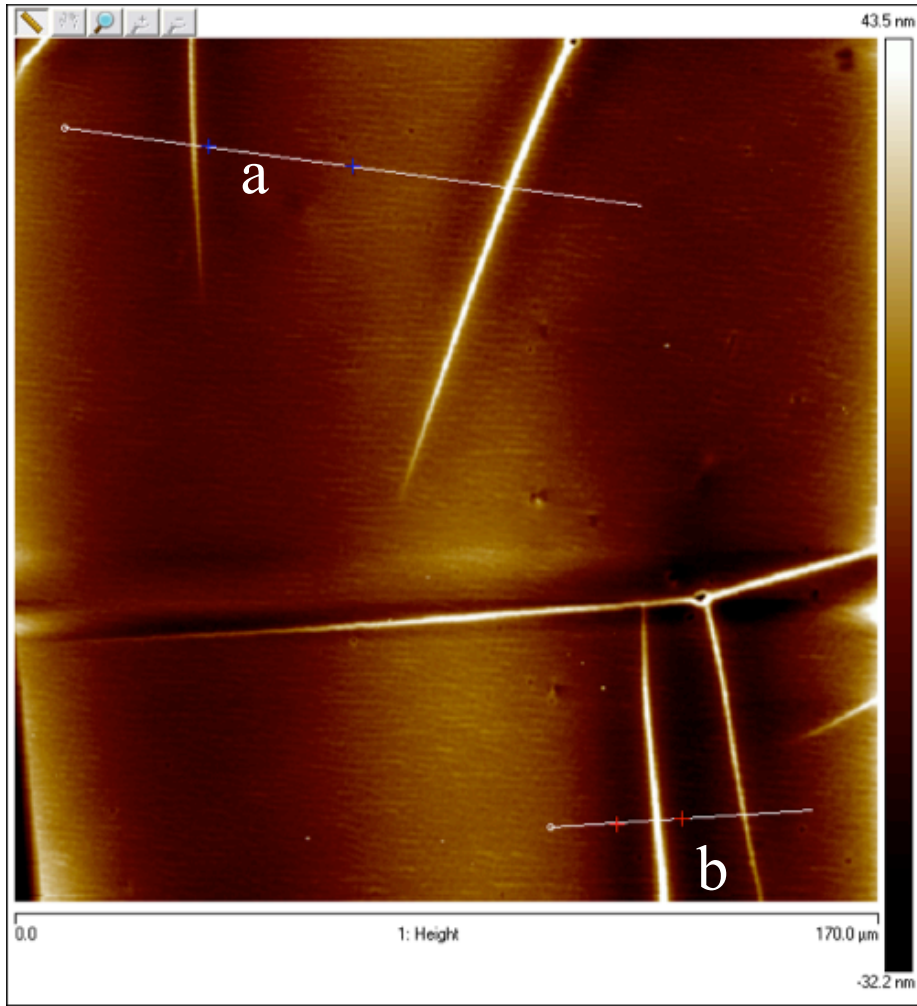


**Figure 5.6-3. AFM height map of PDMS stamp surface. The master mould is a 3.2  $\mu\text{m}$  thick SU-8 5 with a 140  $\text{mJ}/\text{cm}^2$  exposure dose.**

The ridges were narrow and had a maximum height of approximately 60 nm (figure 5.6-4). Its occurrence corresponded to cracks that had been observed in the photoresist film.

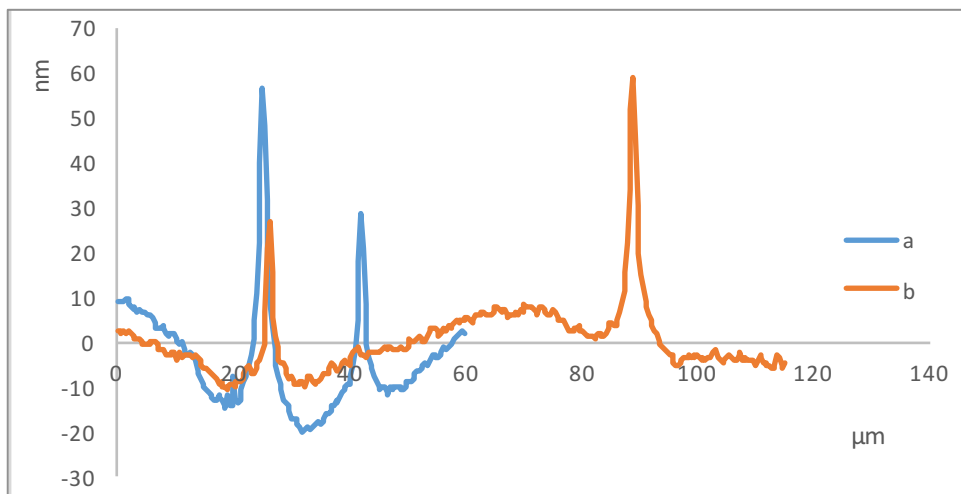


**Figure 5.6-4. Height (nm) and separation ( $\mu\text{m}$ ) of features on PDMS stamp surface.**

The PDMS stamp from the master mould exposed at  $120 \text{ mJ/cm}^2$  showed some regular patterning on the surface, indicating that the square patterned had been successfully transferred to the elastomer (figure 5.6-5).

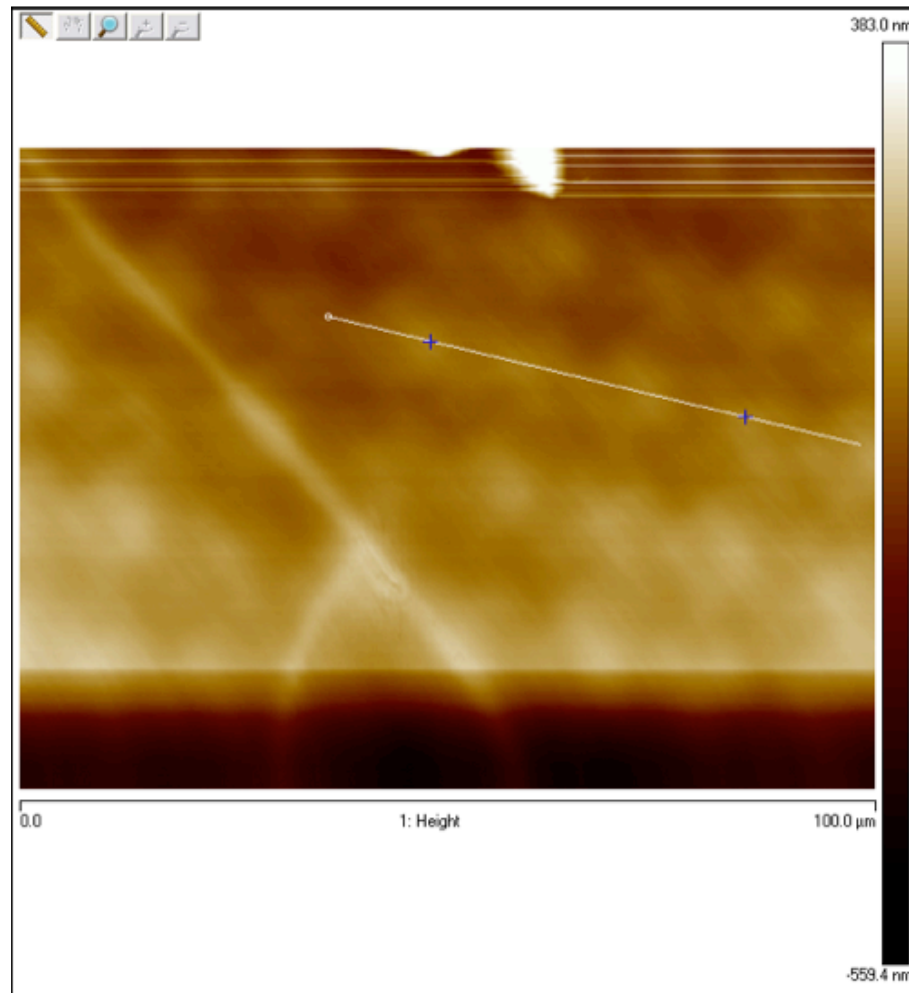


**Figure 5.6-5. AFM height map of 6x6  $\mu\text{m}$  squares patterned PDMS stamp.** The master mould was a  $3.2 \mu\text{m}$  layer of SU-8 5 on a 4" silicone wafer.

The AFM analysis showed that the height and width of these features was fairly constant across the stamp surface, but that the maximum height was only around 60 nm (figure 5.6-6). This was lower than expected based on the measured film thickness.

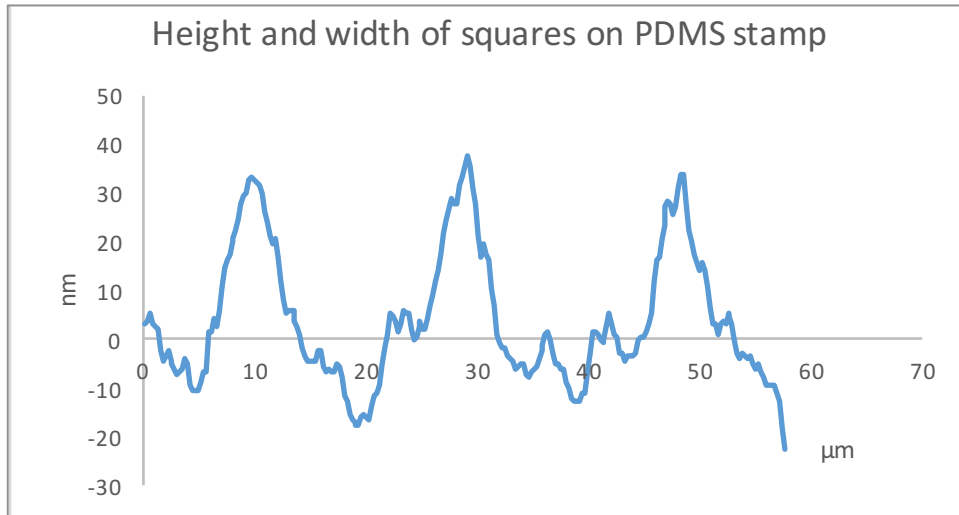


**Figure 5.6-6. Height (nm) and vertical distance (μm) between features on a PDMS stamp.**

The shape of the features appeared somewhat irregular, indicating that the tops of the structures were not completely flat and even (figure 5.6-7). This could also contribute to poor conformal contact between the stamp and substrate surface.

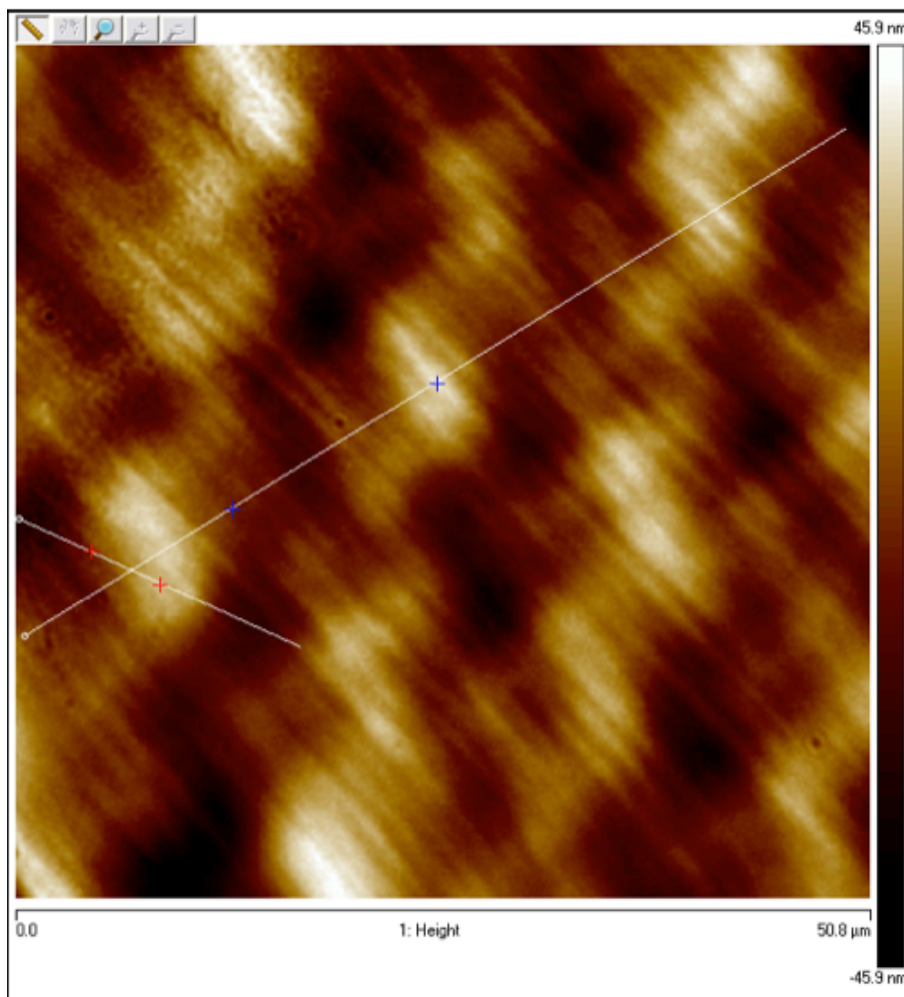


**Figure 5.6-7. AFM height map of 6x6 μm squares patterned PDMS stamp.** The master mould was a 3.2 μm layer of SU-8 5 on a 4" silicone wafer.

The measured feature height does show a degree of regularity over this area of the stamp (figure 5.6-8). Height and width is measured along the line indicated in figure 5-19. The maximum height of the features was observed to be approximately 100 nm, but there was some significant variation in feature size that would prevent successful  $\mu$ CP.

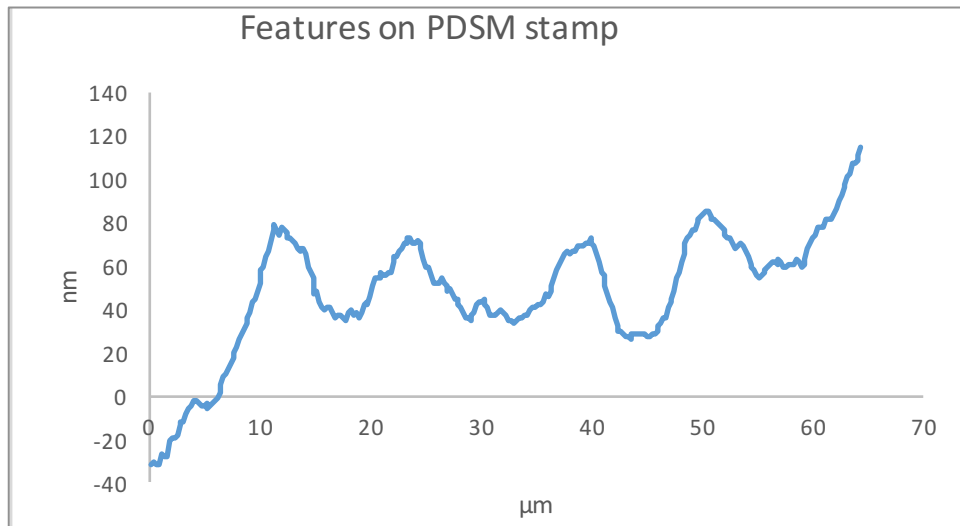


**Figure 5.6-8. Height (nm) and vertical distance ( $\mu\text{m}$ ) between features on a PDMS stamp.**

The AFM analysis showed that there was a regular pattern present on the stamp surface after the  $120 \text{ mJ}/\text{cm}^2$  exposure dose. The designed pattern was transferred from the master mould to the PDMS pattern, and some regularity of pattern was observed. Analysis also showed ridges in the pattern, corresponding to the cracks observed in the resist surface. The height of the ridges explained why poor contact between the stamp surface and the substrate was achieved. The ridge would come into contact with the surface first and prevent the pattern from touching the glass surface evenly. Height is even along the entire ridge, indicating that there was an even resist thickness across the substrate.

The observed feature size was smaller than the measured film thickness ( $\sim 3.8 \mu\text{m}$ ), indicating that parts of the photoresist that additional areas dissolved during development. The observed cracks were irregular, which explains why some parts of the pattern are reproduced while others are not. It was difficult to study the stamps with the AFM due to the placement of arrays at the edge of sample cuts from the stamp combined with the stamp thickness. Further AFM analysis of smaller stamp cut-outs might be able to give more insight into the irregularities.

### 5.6.1. Immobilization of *S. cerevisiae*

*S. cerevisiae* was successfully immobilized on surfaces functionalized with PLL (0.01%). An even coating of *S. cerevisiae* was achieved across the surface (figure 5.6-9), replicating the results achieved by Åshild Samseth (44).

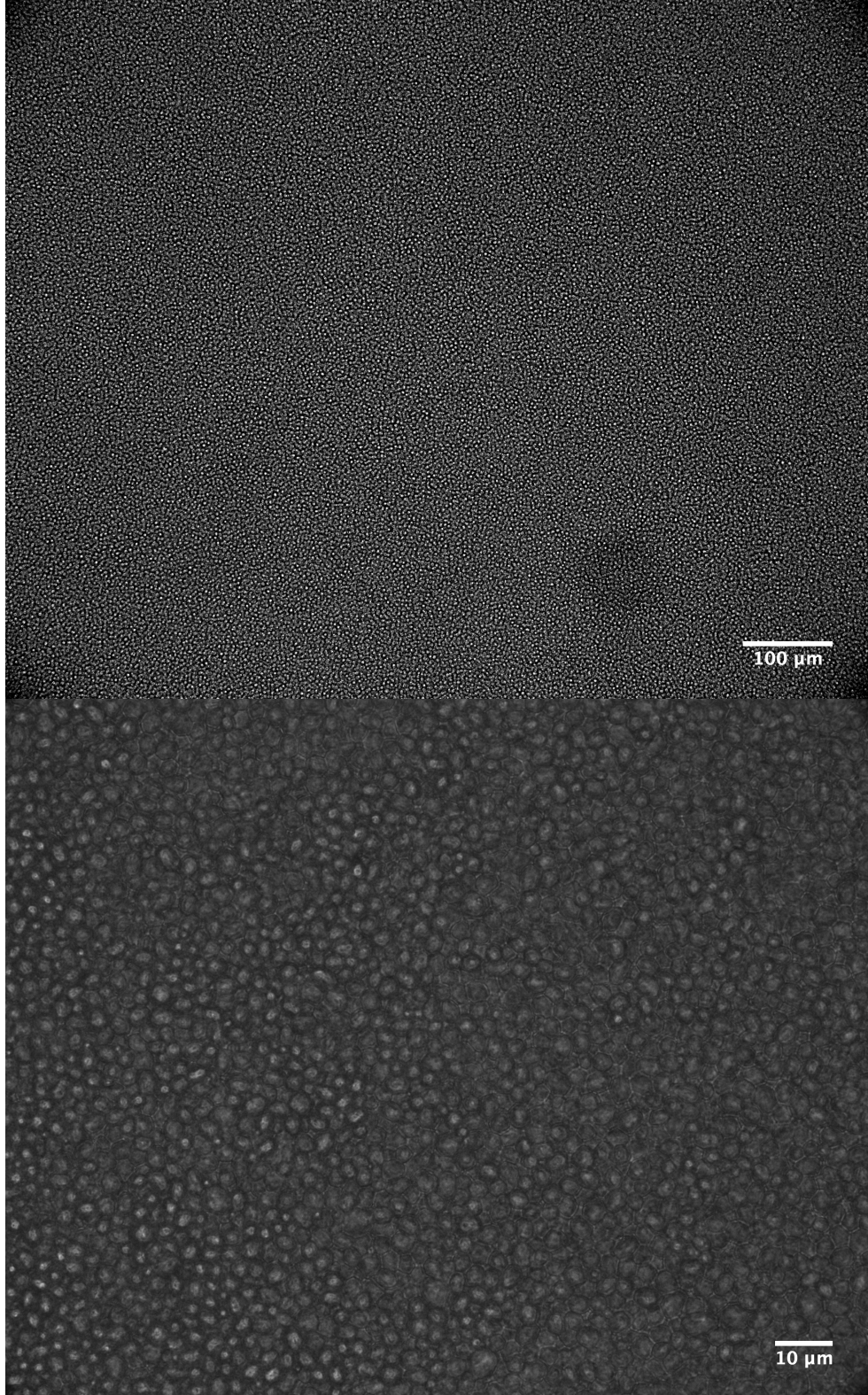


Figure 5.6-9. *S. cerevisiae* immobilized on a glass surface functionalized with PLL (0.01%).

Studying the sample underneath the microscope revealed that all the immobilized cells were in the same layer, indicating that the cells only adhere to the PLL and not to each other. The non-functionalized areas of the glass did not have cells on them after cleaning, indicating that a passivation agent is not needed for work with *S. cerevisiae*.

*S. cerevisiae* was also attempted immobilized on areas of PLL-FITC deposited by  $\mu$ CP. However, application of the yeast cell solution to the adhesive islands caused detachment from the glass surface. Yeast cells attached to the PLL-FITC and became fluorescently tagged, but were not immobilized. The PLL-FITC had a similar chain length as the PLL used for successful immobilization of yeast cells on a non-patterned surface. A possible explanation for the observed difference was the effect of the attached FITC tag, which could have influenced the adhesive characteristics of the molecule.

## 6. Conclusion and outlook

A method for  $\mu$ CP of PLL in a micrometre scale pattern was established using PDMS stamps. PLL-FITC was used to verify that PLL could be stamped in a microscale pattern using  $\mu$ CP. Structures down to 0.8  $\mu\text{m}$  spots were successfully printed on glass surfaces. The patterns were inspected using fluorescence microscopy with a Zeiss AxioCam Z.1 microscope. It was successfully demonstrated that plasma cleaning of the PDMS stamps improved the quality of  $\mu$ CP when compared to non-treated stamps. The study was also able to reproduce results showing that *S. Cerevisiae* can be immobilized on a glass surface functionalized with a layer of non-patterned PLL. The immobilized cells remained in place when flushing with DI water or yeast growth medium.

Spin parameters for the photoresist SU-8 5 were optimized and a stable film thickness of approximately 3.8  $\mu\text{m}$  was achieved. The presence of an edge bead was reduced significantly by increasing the spin speed. However, the development of cracks in the resist film during PEB was not resolved during the project. It was determined that the PEB was the critical step for crack formation and it has been suggested that a lowered PEB temperature could reduce the problem.

The presence of the edge bead is also assumed to reduce the quality of the resist film and thus contribute to the cracking. As the edge bead interferes with the contact between mask and substrate, it results in an uneven exposure of the resist film giving varied degrees of cross-linking across the surface. This could make the film more vulnerable to thermal stress. AFM analysis of the PDMS stamps showed ridges across the pattern corresponding to the cracks observed in the resist film. The appearance of the ridges explained the partial printing achieved when attempting  $\mu$ CP with the stamps produced, as the ridges prevented conformal contact between the stamp surface and the substrate.

Further AFM studies of the stamp surfaces could be performed to better characterize the irregularities of the surface. The shape of the features should also be characterized more closely to see whether they are flat or have a more rounded shape that would decrease the possibility of conformal contact. While further optimization of the PEB conditions and edge bead removal steps could be added to the lithography procedure to improve the results, I would suggest taking a step back and re-starting the process with a different resist. The

problems experienced have been particular to the chosen resist and it appears more beneficial to create a procedure for a different resist rather than spending more time and resources on trying to reduce the problems with SU-8 5.

Once a lithography procedure is in place, it would be interesting to study immobilization of *S. cerevisiae* on a patterned surface to find whether there are significant differences compared to a layer of PLL. If immobilization on a pattern is achieved, the next logical step would be creating a pattern that facilitates adhesion of single cells. Parameters that would need to be studied for SCA include size of the adhesive islands as well as separation distance.



## Bibliography

1. Ockenga W. A Brief History of Light Microscopy – From the Medieval Reading Stone to Super-Resolution 2015 [updated September 08, 2015]. Available from: <http://www.leica-microsystems.com/science-lab/history/a-brief-history-of-light-microscopy-from-the-medieval-reading-stone-to-super-resolution/>.
2. Wang D, Bodovitz S. Single cell analysis: the new frontier in 'omics'. *Trends Biotechnol.* 2010;28(6):281-90.
3. Yin H, Marshall D. Microfluidics for single cell analysis. *Current Opinion in Biotechnology.* 2012;23(1):110-9.
4. Arnfinnsdottir NB, Ottesen V, Lale R, Sletmoen M. The Design of Simple Bacterial Microarrays: Development towards Immobilizing Single Living Bacteria on Predefined Micro-Sized Spots on Patterned Surfaces. *PLOS ONE.* 2015;10(6):e0128162.
5. Whitesides GM, Ostuni E, Takayama S, Jiang X, Ingber DE. Soft lithography in biology and biochemistry. *Annual review of biomedical engineering.* 2001;3:335-73.
6. Francois JM, Formosa C, Schiavone M, Pillet F, Martin-Yken H, Dague E. Use of atomic force microscopy (AFM) to explore cell wall properties and response to stress in the yeast *Saccharomyces cerevisiae*. *Current Genetics.* 2013;59(4):187-96.
7. Dague E, Jauvert E, Laplatine L, Viallet B, Thibault C, Ressler L. Assembly of live micro-organisms on microstructured PDMS stamps by convective/capillary deposition for AFM bio-experiments. *Nanotechnology.* 2011;22(39):395102.
8. Mele E, Pisignano D. Nanobiotechnology: Soft Lithography. In: Müller WEG, Grachev MA, editors. *Biosilica in Evolution, Morphogenesis, and Nanobiotechnology: Case Study Lake Baikal.* Berlin, Heidelberg: Springer Berlin Heidelberg; 2009. p. 341-58.
9. Qin D, Xia Y, Whitesides GM. Soft lithography for micro- and nanoscale patterning. *Nat Protocols.* 2010;5(3):491-502.
10. Alom Ruiz S, Chen CS. Microcontact printing: A tool to pattern. *Soft Matter.* 2007;3(2):168-77.
11. Altschuler SJ, Wu LF. Cellular Heterogeneity: Do Differences Make a Difference? *Cell.* 141(4):559-63.
12. Brooks Michael D, Burness Monika L, Wicha Max S. Therapeutic Implications of Cellular Heterogeneity and Plasticity in Breast Cancer. *Cell Stem Cell.* 17(3):260-71.
13. Arias CA, Murray BE. Antibiotic-Resistant Bugs in the 21st Century — A Clinical Super-Challenge. *New England Journal of Medicine.* 2009;360(5):439-43.
14. Heath JR, Ribas A, Mischel PS. Single-cell analysis tools for drug discovery and development. *Nat Rev Drug Discov.* 2016;15(3):204-16.
15. Toriello NM, Douglas ES, Thaitrong N, Hsiao SC, Francis MB, Bertozzi CR, et al. Integrated microfluidic bioprocessor for single-cell gene expression analysis. *Proceedings of the National Academy of Sciences.* 2008;105(51):20173-8.
16. Le Gac S, van den Berg A. Single cells as experimentation units in lab-on-a-chip devices. *Trends in Biotechnology.* 2010;28(2):55-62.
17. Théry M. Micropatterning as a tool to decipher cell morphogenesis and functions. *Journal of Cell Science.* 2010;123(24):4201-13.
18. Bernard A, Renault JP, Michel B, Bosshard HR, Delamarche E. Microcontact Printing of Proteins. *Advanced Materials.* 2000;12(14):1067-70.
19. Xia Y, Whitesides GM. Self-assembled Monolayer Films: Microcontact Printing A2 - Buschow, K.H. Jürgen. In: Cahn RW, Flemings MC, Ilshner B, Kramer EJ, Mahajan S, Veyssi re P, editors. *Encyclopedia of Materials: Science and Technology (Second Edition).* Oxford: Elsevier; 2001. p. 8309-14.

20. Xu H, Huskens J. Versatile Stamps in Microcontact Printing: Transferring Inks by Molecular Recognition and from Ink Reservoirs. *Chemistry – A European Journal*. 2010;16(8):2342-8.
21. Dow Corning. Sylgard® 184 Silicone Elastomer 2014 [updated 02.04.2014. Available from: <http://www.dowcorning.com/DataFiles/090276fe80190b08.pdf>.
22. Schmid H, Michel B. Siloxane Polymers for High-Resolution, High-Accuracy Soft Lithography. *Macromolecules*. 2000;33(8):3042-9.
23. Murray LM, Nock V, Evans JJ, Alkaisi MM. Bioimprinted polymer platforms for cell culture using soft lithography. *Journal of Nanobiotechnology*. 2014;12(1):60.
24. Renault JP, Bernard A, Bietsch A, Michel B, Bosshard HR, Delamarche E, et al. Fabricating Arrays of Single Protein Molecules on Glass Using Microcontact Printing. *The Journal of Physical Chemistry B*. 2003;107(3):703-11.
25. Bhave G, Gopal A, Hoshino K, Zhang JX. Microcontact Printing. In: Bhushan B, editor. *Encyclopedia of Nanotechnology*. Dordrecht: Springer Netherlands; 2014. p. 1-12.
26. Microchemicals. Resists, Developers and Removers 2017 [updated 07.11.13. Available from: [http://www.microchemicals.com/downloads/application\\_notes.html](http://www.microchemicals.com/downloads/application_notes.html).
27. Microchemicals. Spin Coating of Photoresists 2013 [updated 07.11.13. Available from: [http://www.microchemicals.com/technical\\_information/spin\\_coating\\_photoresist.pdf](http://www.microchemicals.com/technical_information/spin_coating_photoresist.pdf).
28. Sahu N, Parija B, Panigrahi S. Fundamental understanding and modeling of spin coating process : A review. *Indian J Phys*. 2009;83(4):493-502.
29. Microchemicals. Photoresist Coating Techniques 2013 [updated 07.11.13. Available from: [http://www.microchemicals.com/technical\\_information/photoresist\\_coating.pdf](http://www.microchemicals.com/technical_information/photoresist_coating.pdf).
30. Microchemicals. NANO(TM) SU-8 Negative Tone Photoresist Formulations 2-25 2002 [updated 2/02. Available from: [http://www.microchem.com/pdf/SU8\\_2-25.pdf](http://www.microchem.com/pdf/SU8_2-25.pdf).
31. Microchemicals. Softbake of Photoresist Films 2013 [updated 07.11.13. Available from: [http://www.microchemicals.com/technical\\_information/softbake\\_photoresist.pdf](http://www.microchemicals.com/technical_information/softbake_photoresist.pdf).
32. Bowen RM. Residual Stress in SU-8 Photoresist Films. Rochester Institute of Technology, Engineering DoM. Report No.: 0305-320.
33. Li B, Liu M, Chen Q. Low-stress ultra-thick SU-8 UV photolithography process for MEMS. *MOEMS*. 2005;4(4):043008--6.
34. Microchemicals. Exposure of Photoresists 2013 [updated 07.11.13. Available from: [http://www.microchemicals.com/technical\\_information/exposure\\_photoresist.pdf](http://www.microchemicals.com/technical_information/exposure_photoresist.pdf).
35. Fucetola CP, Carter DJD, Goodberlet JG. Exposure latitude of deep-ultraviolet conformable contact photolithography. *Journal of Vacuum Science & Technology B: Microelectronics and Nanometer Structures Processing, Measurement, and Phenomena*. 2008;26(1):36-40.
36. Süss Microtech AG. MA/BA6 Mask and Bond Aligner [cited 2017 10.05.17]. Available from: <https://www.suss.com/en/products-solutions/mask-aligner/ma-ba-6>.
37. Stephan K, Gabriela B, Michael L, Daniel H, Anja B. Processing of thin SU-8 films. *Journal of Micromechanics and Microengineering*. 2008;18(12):125020.
38. Ou J, Glawdel T, Ren CL, Pawliszyn J. Fabrication of a hybrid PDMS/SU-8/quartz microfluidic chip for enhancing UV absorption whole-channel imaging detection sensitivity and application for isoelectric focusing of proteins. *Lab Chip*. 2009;9(13):1926-32.
39. Lesage G, Bussey H. Cell Wall Assembly in *Saccharomyces cerevisiae*. *Microbiology and Molecular Biology Reviews*. 2006;70(2):317-43.
40. Boorsma A, Nobel Hd, Riet Bt, Bargmann B, Brul S, Hellingwerf KJ, et al. Characterization of the transcriptional response to cell wall stress in *Saccharomyces cerevisiae*. *Yeast*. 2004;21(5):413-27.

41. Orlean P. Architecture and Biosynthesis of the *Saccharomyces cerevisiae* Cell Wall. *Genetics*. 2012;192(3):775-818.
42. Klis FM, Mol P, Hellingwerf K, Brul S. Dynamics of cell wall structure in *Saccharomyces cerevisiae*. *FEMS Microbiology Reviews*. 2002;26(3):239-56.
43. Mirtič A, Grdadolnik J. The structure of poly-l-lysine in different solvents. *Biophysical Chemistry*. 2013;175–176:47-53.
44. Samseth Å. Immobilisering av *Saccharomyces Cerevisiae* og virkning av kitosan på den mekaniske styrken til celleveggen til *Saccharomyces Cerevisiae* [Master thesis]. Trondheim: NTNU; 2016.
45. Choi J-H, Kim S-O, Linardy E, Dreaden EC, Zhdanov VP, Hammond PT, et al. Influence of pH and Surface Chemistry on Poly(l-lysine) Adsorption onto Solid Supports Investigated by Quartz Crystal Microbalance with Dissipation Monitoring. *The Journal of Physical Chemistry B*. 2015;119(33):10554-65.
46. Mazia D, Schatten G, Sale W. Adhesion of cells to surfaces coated with polylysine. Applications to electron microscopy. *The Journal of cell biology*. 1975;66(1):198-200.
47. Aguilar-Uscanga B, François JM. A study of the yeast cell wall composition and structure in response to growth conditions and mode of cultivation. *Letters in Applied Microbiology*. 2003;37(3):268-74.
48. Sletmoen M, Davies CdL, Psonka-Antonyczyk KM, Stokke BT. *Biphsical Nanotechnologies: lecture notes for the PhD course in Light and force based molecular imaging*. Trondheim: NTNU2011.
49. Alberts B, Johnson A, Lewis J, Raff M, Roberts K, Walter P. *Molecular Biology of the Cell*. 5 ed. New York: Garland Science, Taylor & Francis Group, LLC; 2008.
50. Pillet F, Chopinet L, Formosa C, Dague E. Atomic Force Microscopy and pharmacology: from microbiology to cancerology. *Biochimica et biophysica acta*. 2014;1840(3):1028-50.
51. Tinku S, Iacob E, Lorenzelli L, Dahiya R. Surface Characterization Of Polydimethylsiloxane: An AFM Study AISEM Annual Conference Trento, Italy2015.
52. Arnfinnsdottir NB. *Microscale tools for the development of bacterial microarrays*. Trondheim: NTNU; 2016.
53. Sigma Aldrich. Kit for PDMS Surface Modification [Available from: <http://www.sigmaaldrich.com/technical-documents/articles/materials-science/microelectronics-nanoelectronics/pdms-surface-modification.html>].